# **Cover Letter**

Dear Dr Rossetti,

In the present version of the paper entitled "Plio-Quaternary tectonic evolution of the southern margin of the Alboran Basin (Western Mediterranean)", several modifications have been made in accordance with the points you raised in your last review.

We modified the Introduction section. It has been shortened and modified to present the scientific problem clearly. We also reorganized the section to avoid the repetitions. In the result section, we modify the text to avoid scientific inferences and moved them into the discussion.

We reorganized and edited the discussion section. Table 1 has been moved to the 15<sup>th</sup> position of the figures. Eventually, we do not change the words 'restraining bend', which is the exact terminology for a compressive relay in between strike-slip fault segments (e.g. Mann, 2007). We modified the text to demonstrate better the transpression. Blocks and basements faults rotation are based on a comparison with analog models and the literature. The last section has been shortened according to previous comments. We modified the figures to be sure that localities are present on the maps.

Overall, we took great attention to the style and have corrected many grammatical mistakes. It results a shorter and clearer paper. We believe that this version is suitable for publication. We also would like to add a co-author (Dr Jeroen Smit) who helped us to reviewed to grammar and the organization of the text during this iteration.

Dr Manfred Lafosse and co-authors.

# Plio-Quaternary tectonic evolution of the southern margin of the Alboran Basin (Western Mediterranean)

Manfred Lafosse<sup>1,\*</sup>, Elia d'Acremont<sup>1</sup>, Alain Rabaute<sup>1</sup>, Ferran Estrada<sup>2</sup>Estrada<sup>3</sup>, Martin Jollivet-5 Castelot<sup>3</sup>Castelot<sup>4</sup>, Juan Tomas Vazquez <sup>45</sup>, Jesus Galindo-Zaldivar <sup>5,6,7</sup>, Gemma Ereilla<sup>2</sup>Ercilla<sup>3</sup>, Belen Alonso<sup>2</sup>Alonso<sup>3</sup>, Jeroen Smit<sup>2</sup>, Abdellah Ammar<sup>7</sup>Ammar<sup>8</sup>, Christian Gorini<sup>1</sup>

<sup>1</sup> Sorbonne Université, CNRS-INSU, Institut des Sciences de la Terre Paris, ISTeP UMR 7193, F-75005 Paris, France <sup>2</sup> Instituto de Ciencias del Mar, ICM CSIC, Continental Margin Group, 08003 Barcelona, Spain

<sup>32</sup>-Univ. Lille, CNRS, Univ. Littoral Côte d'Opale, UMR 8187, Labratoire d'Océanologie et de Géosciences (LOG), F59000,
 10 Lille, France

<sup>4</sup> Instituto Espanol de Oceanografia, C.O.Malaga, Fuengirola, Spain <sup>5</sup> Dpto. de Geodinamica, Universidad de Granada, Granada, Spain. <sup>6</sup> Instituto Andaluz de Ciencias de la Tierra (CSIC UGR), Granada, Spain. <sup>7</sup> Université Mohammed V Agdal, Rabat, Morocco

15 \*now at: Tectonic and Structural Geology Groups, Department of Earth Sciences, Utrecht University, PO Box 80.021, 3508 TA Utrecht, The Netherlands

<sup>3</sup> Instituto de Ciencias del Mar, ICM-CSIC, Continental Margin Group, 08003 Barcelona, Spain

<sup>4</sup> <u>Univ. Lille, CNRS, Univ. Littoral Côte d'Opale, UMR 8187, Labratoire d'Océanologie et de Géosciences (LOG), F59000,</u> <u>Lille, France</u>

- <sup>5</sup> Instituto Espanol de Oceanografia, C.O.Malaga, Fuengirola, Spain
   <sup>6</sup> Dpto. de Geodinamica, Universidad de Granada, Granada, Spain.
   <sup>7</sup> Instituto Andaluz de Ciencias de la Tierra (CSIC-UGR), Granada, Spain.
   <sup>8</sup> Université Mohammed V-Agdal, Rabat, Morocco
- 25 Correspondence to: Manfred Lafosse (m.r.lafosse@uu.nl)

Abstract. <u>ProgressesProgress</u> in the understanding and dating of the sedimentary record of the Alboran Basin <u>allowallows</u> us to propose a model of the evolution of its tectonic evolution since the Pliocene-to the present time. After a period of extension, the Alboran Basin <u>undergoesunderwent a</u> progressive tectonic inversion since 9 - 7.5 Ma. The Alboran Ridge is a NE-SW transpressive structure accommodating the shortening in the basin. We <u>mapmapped</u> its southwestern termination: a Pliocene

- 30 rhombic structure exhibiting series of folds and thrusts. The <u>active Al-Idrissi fault zone</u> (AIF) is a <u>youngerPleistocene</u> strikeslip structure <u>withtrending NNE-SSW-strike</u>. The AIF an active fault zone, which crosses the Alboran Ridge and connects southward to the transtensive Nekor Basin and the Nekor fault. In the Moroccan shelf and at the edge of a submerged volcano, we <u>datedated</u> the inception of the local <u>shelf</u> subsidence <u>fromat</u> 1.81-1.12 Ma. <u>ItThe subsidence</u> marks the propagation of the AIF toward the Nekor Basin. Pliocene thrusts and folds and Quaternary transtension appear at first sight
- 35 asto act at different tectonic periods but reflectsreflect the long-term evolution of a transpressive system. Despite athe constant direction of Africa/Eurasia convergence since 56 Ma-at the scale of, along the southern margin of the Alboran Basin, the Pliocene-Quaternary compression evolves from transpressive to transtensive onalong the AIF and the Nekor Basin. This

system <u>can reflectreflects</u> the <u>expectedlogical</u> evolution of the deformation of the Alboran Basin under the indentation of the African lithosphere.

40

#### 1. Introduction

In a brittle regime, oblique compression leads to strain partitioning between lateral motion and efficient rock uplifts (Fossen et al., 1994; Fossen and Tikoff, 1998). With time, the simple shear deformation involves blocks rotation and changes in the local stress field, leading to the formation of better oriented tectonic structures (Nur et al., 1986; Ron et al., 2001; Scholz et

- 45 al., 2010). It often results in an intricate pattern of distributed deformation with transpressive and transtensive structures. The Alboran Basin could be a typical example of such a complex tectonic evolution.
  - The Alboran Basin develops over a collapsed Tertiary orogen and is limited onshore by the Betic Rif belt (Fig. 1) (Comas et al., 1999). The formation of the Alboran Basin has been linked to back arc extension during early Miocene (e.g., Jolivet et al., 2009, 2008). Since the Miocene, several strike slip shear zones running from the Iberian to the Moroccan margins
- 50 accommodate the upper plate deformation forming a broad shear zone called the Trans Alboran Shear Zone (TASZ; Fig. 1)(Leblanc and Olivier, 1984). Following the westward slab retreat, the TASZ behaves as a left lateral transfer fault zone accommodating the extension of the Alboran Basin. The Africa Eurasia NW SE oblique convergence leads to a tectonic reorganization during the Late Miocene (Comas et al., 1999; Do Couto et al., 2016). Due to ongoing Africa Eurasia convergence, the TASZ underwent an oblique positive inversion starting around 8 Ma in the Betic Margin of the Sorbas Basin
- 55 (Do Couto et al., 2014; Martínez García et al., 2017). The compression migrates westward since approximately 7-8 Ma from the Algerian margin to the Alboran Ridge, and since ca. 5 Ma on the Al Idrissi fault (Fig. 1 and 2) (Giaconia et al., 2015). The Plio-Quaternary tectonics of the Alboran Basin and its margins show the superposition of transpressive and transtensive structures that have been attributed to different mechanisms including chances in far field-stress, slab roll-back and mantle delamination (Calvert et al., 2000; Gutscher et al., 2002; Martínez-García et al., 2013, 2017; Petit et al., 2015; Thurner et al.,
- 60 2014). At present day, GPS velocities define an Alboran tectonic domain in between Africa and Iberia rigid blocks (Fig. 1) (Neres et al., 2016; Palano et al., 2013, 2015). Based on the seismicity (Fig. 2), a present-day diffuse plate boundary between Africa and Eurasia was proposed in the Alboran Basin and the Betic-Rif belt (Bird, 2003; Neres et al., 2016; Palano et al., 2015). DeMets et al. (2015) very precisely constrained the location of the rotation poles between Eurasia, North America, and Africa since the Miocene. They show that since 5.2 Ma, the southeastward migration of the rotation pole between Africa and
- 65 Eurasia results in a roughly constant direction of convergence and an increase in the convergence rate (from ~3.5 mm/y to ~5.5 mm/y at 35° N / 5° W). More recently, Spakman et al., (2018) show that from 8 Ma to present-day, the Africa Eurasia absolute convergence has produced 15km of relative motion in the NNE-SSW direction. This questions the idea of a change in plate kinematics as the cause for changes of tectonic evolution in the Alboran tectonic domain (Martínez-García et al., 2013).

Lithosphere-scale processes and crustal heterogeneities such as mantle and lower crustal delamination have a strong influence

70 on the deformation and the structure of the Alboran Basin (Petit et al., 2015; Thurner et al., 2014).

Several authors shows the moderate oblique convergence relatively to the principal tectonic structures of the TASZ. DeMets et al. (2015) showed that it is possible to constraint very precisely the location of the rotation poles between Eurasia, North America, and Africa since the Miocene. The migration of the rotation pole between Africa and Eurasia toward the SE during the Pliocene and the Quaternary results in a roughly constant direction of Africa Eurasia convergence, an increase in the

75 convergence rates from approximately ~3.5 mm/y to ~5.5 mm/y at 35° N / 5° W between 5.2 Ma and present day, respectively (DeMets et al., 2015). The mechanical coupling between the Alboran Domain and the subsiding lithosphere, and/or slab dragging under Africa/Eurasia convergence could cause the extrusion of the Betic-Rif belt toward the South-West (Neres et al., 2016; Perouse et al., 2010; Petit et al., 2015; Spakman et al., 2018; Thurner et al., 2014).

<u>Plio-Quaternary-More recently, Spakman et al., (2018) show that from 8 Ma to present day, the Africa – Eurasia absolute</u>
 convergence-produces 15km of relative motion between Africa and Eurasia in the NNE SSW direction.

- However, changes in stress direction are<u>directions have been</u> demonstrated in the Betic-Rif belt during the Plio-Quaternaryfrom field geology, (Aït Brahim and Chotin, 1990; Galindo-Zaldívar et al., 1993; Giaconia et al., 2015; Martínez-Díaz and Hernández-Enrile, 2004). In the Rif, field studies and paleomagnetic data demonstrate a 20° counter clock wise rotation since the upper Miocene (Crespo Blanc et al., 2016; Platt et al., 2003). The change in horizontal stress directions
- 85 has The local changes in horizontal stress directions have led to compression and uplift of Plio-Quaternary sediments offshore the Palomares fault on the Iberian Margin (Giaconia et al., 2015). At present time, the direction of shortening seems orthogonal to the NE-SW structures of the TASZ (Fig. 1)(Palano et al., 2013). In the Rif, field studies and paleomagnetic data demonstrated a 15° counter clock-wise rotation since the upper-Miocene (Crespo-Blanc et al., 2016, and references therein). At presenttime, the direction of shortening seems to be orthogonal to the offshore NE-SW Trans Alboran Shear Zone (TASZ) (Fig. 1)
- 90 (Palano et al., 2013). Recent structural mapping has shown that the offshore distribution of the deformation in the Alboran Sea has localized during the Quaternary on a set of conjugated strike-slip faults: the Al-Idrissi Fault (AIF) and the Averroes Fault (Fig. 1) (Estrada et al., 2018; Galindo-Zaldivar et al., 2018; Lafosse et al., 2017; Martínez-García et al., 2013, 2017). Along the newly formed Averroes Fault (Fig. 1), the onset of the strike-slip motion has been estimated around 1 Ma (Perea et al., 2018). Using a block rotation pinned model, Meghraoui and Pondrelli, (2013) proposehave proposed that the oblique
- 95 convergence leadsled to a rigid-\_block rotation accommodated by transcurrent faults (e.g. the TASZ, Fig. 1). <u>However, the timing and mechanism of this structural evolution remains poorly constrained.</u> Besides, the distribution of the seismicity in the western part of the Betic-Rif belt reveals complex geodynamic interactions.

Deep earthquakes occur at depths >60 km (Fig. 2a). They are located in the central Betic, beneath the West Alboran Basin (WAB), and the Rif Mountains ( Fig. 1), and are associated to a sinking slab (Fig. 2a) (Bezada et al., 2013; Ruiz Constán et

100 al., 2011; Thurner et al., 2014). In addition to the Africa-Eurasia convergence, lithospheric scale processes and crustal heterogeneities such as mantle and lower crust delamination can have a strong influence on the deformation and the structure of the Alboran Basin (Petit et al., 2015; Thurner et al., 2014). The mechanical coupling between the Alboran Domain and the

subsiding lithosphere (e.g. Perouse et al., 2010; Neres et al., 2016), and/or slab dragging under Africa/Eurasia convergence (Spakman et al., 2018) could cause the extrusion of the Betico Rifian belt toward the South West (e.g. Petit et al., 2015;

105 Thurner et al., 2014).

The Africa Eurasia plate boundary in the Alboran Basin and the Betic – Rif belt cannot be assigned to a single fault system (Fadil et al., 2006), and some authors proposed to define a present day diffuse plate boundary between Africa and Eurasia (e.g., Palano et al., 2015). At the crustal level, recent progress in structural mapping have shown that the distribution of the deformation in the Alboran Sea switched from the Tortonian NE SW to Quaternary NNE SSW faults (Estrada et al., 2018;

110 Galindo Zaldivar et al., 2018; Lafosse et al., 2017; Martínez García et al., 2013, 2017). On the Averroes Fault (Fig. 1), the estimate of the age of strike slip deformation is around 1Ma (Perea et al., 2018). However, the timing and the mechanism of this structural evolution remains poorly constraint.

In the present work, we address the <u>Plio-Quaternary</u> structural evolution of the southwestern margin of the Alboran Basin, toward the southern termination of the <u>TASZ</u> through the <u>Plio Quaternary</u>. We analyze Trans Alboran Shear Zone. In this

- 115 poorly studied, yet key region, we analyze in high-resolution the changes of tectonic and stratigraphic setting by the means of newly acquired multi-resolution 2D seismic reflection data, and TOPAS profiles, and multibeam data. Based on the seismic stratigraphic interpretation of our recent datasetdatabase and our seismic stratigraphic interpretation a regional synthesis of structural data, we observe propose that the structural subdivision volution of the Alboran Basin and its southern margin may reflect reflects a Pleistocene change in tectonic style. We propose aOur new tectonic model explaining explains the evolution
- 120 of the SAR and the Al-Idrissi fault Zone in the southern margin of the Alboran Basin and the Al-Idrissi fault Zone during the constant Africa/Eurasia convergence.

#### 1.1. Geological and geodynamical settings

In the southern margin of the Alboran Sea, the main structural element corresponds to the Alboran Ridge. It corresponds to a tectonic high building upThe Alboran Basin developed over a collapsed Tertiary orogen and is limited onshore by the BeticRif belt (Fig. 1) (Comas et al., 1999). The formation of the Alboran Basin has been linked to early Miocene forearc extension (Booth-Rea et al., 2007; Faccenna et al., 2001; Jolivet et al., 2008, 2009; Jolivet and Faccenna, 2000; Peña et al., 2018). Several Miocene strike-slip shear zones cross the entire basin from the Iberian to the Moroccan margins and accommodate the upper-plate deformation that form a broad shear zone called the Trans-Alboran Shear Zone (TASZ; Fig. 1) (Leblanc and Olivier, 1984). Following the westward slab retreat, the TASZ acted as a left-lateral fault zone accommodating the extension of the
Alboran Basin. The Africa-Eurasia NW-SE oblique convergence led to a tectonic reorganization during the Late Miocene

(Comas et al., 1999; Do Couto et al., 2016). Due to ongoing Africa-Eurasia convergence, the TASZ underwent an oblique positive inversion starting around 8 Ma in the Sorbas Basin of the Betic Margin (Do Couto et al., 2014; Martínez-García et al., 2017). The compression migrates westward since approximately 7-8 Ma from the Spanish and Algerian margin to the Alboran Ridge, and since *ca.* 5 Ma on the Al-Idrissi fault (Fig. 1 and 2) (Giaconia et al., 2015).

- In the southern margin of the Alboran Sea, the Alboran Ridge corresponds to a tectonic high that developed since the Late-Miocene (Bourgois et al., 1992; Do Couto, 2014). The Alboran Ridge divides the Alboran Basin into three different subbasins: the Western Alboran Basin (WAB), the South Alboran Basin (SAB), and the East Alboran Basin (EAB) (Fig. 1). Transpressive and transtensive structures associated with the Alboran Ridge and the Yusuf fault zone, respectively, as well as to several volcanic or metamorphic highs limit those sub-basins (Fig. 1). The Alboran Ridge is divided by the AIF (Fig. 1) into
  the South Alboran Ridge (SAR, Fig. 1), which corresponds to the submarine highs striking in the NE-SW direction (Xauen Bank, Petit Tofino Bank, Tofino bank, Ramon Margalef High, Eurofleet High, Francesc Pages High, Fig. 3) and the North Alboran Ridge (NAR; Fig 1). The Alboran Ridge and the Yusuf fault divide the Alboran Ridge, the right-lateral Yusuf fault zone is active since the Miocene (Fig. 1) (Martínez-García et al., 2013, 2017). The Al-Idrissi fault divides the Alboran
- 145 Ridge into the North (NAR) and South Alboran (SAR) Ridges (Fig. 1). The SAR corresponds to a series of NE-SW striking submarine highs culminating around -110m (Xauen Bank, Petit Tofino Bank, Tofino bank, Ramon Margalef High, Eurofleet High, Francesc Pagès Bank, Fig. 3).

Sedimentary processes shape the seafloor and control the stratigraphy. On both flanks of the Alboran Ridge, the contourite deposits produce significant thickness variations of the Quaternary depositional units, Sedimentary processes, volcanism and

- 150 tectonics shaped the morphology of the Alboran Ridge. -that are pinched and thinned toward the foot of the submarines highs (Juan et al., 2016).-Above the Messinian Erosional Surface (MES) (Estrada et al., 2011; Garcia-Castellanos et al., 2011), the deep sedimentation in the Alboran Sea is driven by contouritic processes that also shape the seafloor since 5.33 Ma (Ercilla et al., 2016; Juan et al., 2016). On both flanks of the Alboran Ridge, contourite deposits produce significant thickness variations of the Quaternary depositional units that are pinched and thinned toward the foot of the submarines highs (Juan et al., 2016).
- 155 Submarine erosion can occur at the moat of the contouritic systems, generally at the foot of the slopes, whereas deposition occurs at deepest locations (Ercilla et al., 2016; Juan et al., 2016).

Volcanism and tectonic deformations also shaped the morphology of the Alboran Ridge. The SAR is 70 km long and SAR corresponds to a series of faults and folds, and to volcanoes affecting the PlioPliocene-Quaternary depositional sequences (Fig. 3). (Bourgois et al., 1992; Chalouan et al., 1997; Gensous et al., 1986; Martínez-García et al., 2013; Muñoz et al., 2008; Tesson

- 160 et al., 1987)-and to a succession of submarine highs culminating around -110m (Fig. 3). The southern front of. To the south, the SAR corresponds to the northern flank offlanks a NE-SW syncline called the South Alboran Trough (Fig. 3). The northern front of the SAR corresponds to and to the north, the Alboran Channel and the WAB (Fig. 3). The SAR marks the southward transition from a-thinned to thickened continental crust-to the north to thick continental crust to the southwest (Díaz et al., 2016). In the WAB, a syn rift sequence is dated from late Aquitanian Burdigalian to theIt is an inherited early Miocene
- 165 extensional structure, that underwent compressive deformation since 8 Ma (Fig. 1) (Do Couto et al., 2016). In the WAB, a syn-rift sequence is dated late Aquitanian–Burdigalian to Langhian (Do Couto et al., 2016). Pre-Messinian deposits are exposed at the seafloor in the core of the anticlinesAt the base of the sedimentary column of the SAR, the seismic reflection data show early to mid-Miocene under-compacted shales deposited during the extensional period (Do Couto, 2014; Do Couto

et al., 2016; Soto et al., 2008). Pre-Messinian deposits are exposed at the seafloor in the cores of the anticlines of the Alboran

- 170 Ridge (Chalouan et al., 2008; Do Couto et al., 2016; Juan et al., 2016; Tesson et al., 1987). Local occurrences of volcanism in the Francesc Pagès Bank and the Ras Tarf are of Miocene and Pliocene age; (Fig. 1 and 3). The volcanism in the Francesc Pagès Bank is not accurately dated (Gill et al., 2004), but the lithology corresponds to basaltic rocks. Basaltic rocks are dated between 9.6 and 8.7 Ma in the same area by Duggen et al., (2004). In the Ras Tarf; (Fig. 3), the volcanism ends around 9Ma9 Ma (El Azzouzi et al., 2014). TheSamples of the Ibn Batouta Sea Mount exhibitscontain 5 Ma old gabbro (Duggen et al., 2014).
- 175 2008). As evidenced by the seismic reflection data, under compacted shales deposited during the early to mid Miocene extensional period are present at the bottom of the sedimentary column west of the SAR (Do Couto, 2014; Do Couto et al., 2016; Soto et al., 2008)(Duggen et al., 2008).

According to Since the Late-Miocene, deformation has migrated from the Eastern Betic Margin toward the SAR in the southwest (Fig. 1) (Giaconia et al., (2015), since the Late Miocene, the deformation has migrated from the Eastern Betic

- 180 Margin toward the South West and the SAR (Fig. 1). Do Couto et al., (2016) proposed that the SAR underwent compressive deformation since 8 Ma in association with the left lateral strike slip of the Carboneras fault zone (Fig. 1). The SAR is an inherited Miocene extensional structure, but E W folds over north and south dipping thrusts accommodate the shortening of the Alboran Basin and demonstrate a tectonic inversion (Fig. 2)(Chalouan et al., 1997). The SAR is being inverted during the Plio-Quaternary along NE-SW trending faults (Fig. 1) (Chalouan et al., 1997). Seismic reflection profiles and well data show
- 185 that the folding continued until the Quaternary in the Francesc Pagès Bank and highlight several erosion periods during Plio-Quaternary time (Galindo-Zaldivar et al., 2018; Tesson et al., 1987). Unconformities and increasing accumulation rates demonstrateindicate three tectonic phases: a tectonic phase-1 dated from 5.33 Ma to 4.57 Ma, a tectonic phase-2 from 3.28 Ma to 2.45 Ma, and a last tectonic phase-3 between 1.81 Ma and 1.19 Ma (Martínez-García et al., 2013). More recently, it has been suggested that the uplift along the Alboran Ridge culminated around 2.45 Ma in response to shortening (Martínez-García
- 190 et al., (2017)- suggest that the uplift along the Alboran Ridge culminated around 2.45 Ma in response to shortening. The most recent deformations involve sinistral motions in recent NNW SSE transtensive fault network, the sinistral Al Idrissi strike slip fault, and the front indentation of the northern part of the Alboran Ridge (Estrada et al., 2018). The AIF is a leftlateral shear zone crossing the NAR and the SAR at the NE tip of the Francèsc Pagès Bank. It connects to the south to the transtensive Nekor Basin (Lafosse et al., 2017), which accommodates the present-day deformation of the southern margin of
- 195 Alboran (Fig. 2 and 3) (Dillon et al., 1980). Bathymetric and seismic reflection data have shown that the deformation along the AIF is accommodated through a series of sinistral NNE SSW strike slip faults segments (Fig. The most recent deformation involves NNW-SSE sinistral transtension from the frontal indentation of the northern part of the Alboran Ridge to the transtensive Nekor Basin via the AIF, across the NAR and the SAR at the NE tip of the Francesc Pagès Bank (Dillon et al., 1980; Estrada et al., 2018; Lafosse et al., 2017). The Nekor Basin accommodates the present-day deformation of the southern
- 200 <u>Alboran margin (Fig. 2 and 3)</u>. <u>Bathymetric and seismic reflection data show that the deformation along the AIF is</u> accommodated by a series of sinistral NNE-SSW strike-slip faults segments (Fig. 1 and 2) (Ballesteros et al., 2008; Martínez-García et al., 2011). The AIF propagated southward during the Quaternary (Ballesteros et al., 2008; Gràcia et al., 2006;</u>

Martínez-García et al., 2011, 2013), connecting to the NNE-SSW active strike-slip faults north of the Al Hoceima region at the Boussekkour—Bokoya fault zone (Fig. 3) (d'Acremont et al., 2014; Calvert et al., 1997; Lafosse et al., 2017).

- 205 At present day, GPS velocities define an Alboran tectonic domain in between African or Iberian rigid blocks (inset Fig. 1)(Grevemeyer et al., 2015; Neres et al., 2016; Palano et al., 2013, 2015). This block is limited eastward by the TASZ and by the Yusuf Fault (Fig. 1 and 2b). East of the TASZ, the region corresponds to the SAB and the Oriental External Rif, which East of the TASZ, the SAB and the Oriental External Rif behave as the African block (Koulali et al., 2011; Vernant et al., 2010). GPS kinematics showsshow a WNW-ESE convergence rate of 4.6mm/y between Africa and Eurasia plates (Nocquet and
- 210 Calais, 2004). From GPS data, the maximumMaximum present-day rates of extrusion of rates of 5.5-6mm/y in the Alboran tectonic domain are close to 5.5 6mm/y measured between the Jebha and Nekor faults and indicate a southwestward lateral escape (Fig. 2b) (Koulali et al., 2011; Vernant et al., 2010). These geodetic data show a maximum southwestward lateral escape localized between the Nekor fault and the SAR Jebha Fault area (Fig. 2b).
- In the SAB, the AIF and the<u>The</u> Nekor Basin, <u>SAR and AIF</u> are affected by significant crustal seismicity (Bezzeghoud and Buforn, 1999; Stich et al., 2005). In the area of the AIF, the earthquakes mainly occur above 30km deep (Buforn et al., 2017). In the Nekor Basin, the seismogenic depth interval is between 0 and 11km depth (Van der Woerd et al., 2014). The 1994 and 2004 earthquakes in the Al Hoceima area reached Mw=6.3 and 5.9, respectively (Fig.<u>The focal mechanisms of</u>-4) (Custódio et al., 2016). On January 25th, 2016, an earthquake further localized in the vicinity of the AIF zone reached Mw=6.3 (Buforn et al., 2017; Medina & Cherkaoui, 2017; Galindo Zaldívar et al., 2018). The focal mechanisms of those three main regional
- 220 earthquakes show sub-vertical nodal planes and a left lateral displacement (Fig. 4) (Bezzeghoud and Buforn, 1999; Biggs et al., 2006; Calvert et al., 1997; El Alami et al., 1998; Hatzfeld et al., 1993; Stich et al., 2005, 2006). <u>At the north border of the Nekor Basin, earthquakes with Mw=6.3 and 5.9 occurred in 1994 and 2004, respectively (Fig. 4) (Custódio et al., 2016). Near the offshore Nekor Basin, close to the Moroccan coast, the NNE-SSW fault tracks identified at the seafloor, in the vicinity of the epicenters, can correspond to the active fault planes deduced from seismological data (d'Acremont et al., 2014; Calvert et al., 2014; Calvert</u>
- al., 1997; Lafosse et al., 2017). On January 25th, 2016, a Mw=6.3 earthquake occurred in the vicinity of the AIF (Buforn et al., 2017; Medina & Cherkaoui, 2017; Galindo-Zaldívar et al., 2018). In the deep basin, the January 25th 2016 earthquake sequence indicates a strike slip style. In the deep basin, the earthquake sequence indicates a strike-slip mode of the AIF, with mainly NNE-SSW left-lateral motion (Ballesteros et al., 2008; Buforn et al., 2017; Galindo-Zaldivar et al., 2018; Martínez-García et al., 2011; Medina and Cherkaoui, 2017). The Alboran Ridge is reactivated near the AIF, as shown by several Several
- compressional focal mechanismsevents with NE-SW nodal planes parallel to the Alboran Ridge thrust axis, and by strike slip focal mechanisms with a left-lateral motion indicate that the Alboran Ridge is locally reactivated (Fig. 4). In the Nekor Basin, the deformation is distributed partitioned into a normal component intoin the center of the basin and a left-lateral component inon its boundaries borders (Fig. 4) (Lafosse et al., 2017). In the SAR, the style of the deformation is unclear, with focal mechanisms showing strike-slip or normal components indiscriminately (Stich et al., 2010). Below the WAB, deep seismicity indicates ongoing necking of sinking lithospheric material (Sun and Bezada, 2020).Below the WAB, deep earthquakes occur at depths >60 km (Fig. 2a) and are associated to the ongoing necking of sinking lithospheric material (Fig. 2a) (Bezada et al., 2010).

<u>2013; Ruiz-Constán et al., 2011; Sun and Bezada, 2020; Thurner et al., 2014).</u> This distributed lithospheric tear could have propagate from the Betic to the WAB (Heit et al., 2017; Mancilla et al., 2015)-, yet the timing and the effect of this tear on the local tectonic is still poorly understood.

#### 240 **2. Material and methods**

#### 2.1. Data

The data used in this study consists of multichannel seismic-profiles, SPARKER and TOPAS profiles, and multibeam bathymetry. They were, acquired during threefour oceanographic surveys (Fig. 3). The seismic reflection data were acquired with a 12-channel-streamer during the 2011\_Marlboro-1 survey-in 2011, as eight NNW-SSE parallel lines crossing the W-E folds of the SAR and two WSW-ENE parallel lines in the southern domain (Fig. 1, 2 and 3). During the SARAS survey in 2012 (d'Acremont et al., 2014; Lafosse et al., 2017; Rodriguez et al., 2017), were obtained3). The 2012 SARAS survey focused on the acquisition of shallow data. SPARKER and TOPAS profiles, multibeam bathymetry and acoustic reflectivity at a 25m/pixel resolution of the deep submarine seafloor were acquired- (Rodriguez et al., 2017). During the MARLBORO-2 survey in 2012 (d'Acremont et al., 2014; Lafosse et al., 2017), SPARKER profiles and shallow multibeam bathymetry at a 5m/pixel resolution were acquired. The bathymetric data from the 2016 INCRISIS survey were also used (Galindo-Zaldivar et al., 2018). AlsoIn addition, we useused a Digital Elevation Model downloaded from the EMODNET data set (http://www.emodnet.eu/) to fill the missing parts of our dataset.

#### 2.2. Methods

We used the seismic reflection and TOPAS data interpretation to perform for the tectonic mapping analysis of the subsurface. 255 At the seafloor, we made a visual recognition of fault scarps using the multibeam bathymetry and the curvature maps. The curvature is known as a relevant parameter to track the fault offsets on 3D seismic section (e.g. Roberts, 2001) and at the seafloor (e.g., Paulatto et al., 2014). The sum of the plan-curvature values was made with the help of ArcGis V10.2 using the focal statistics tool to smoothen the noise at depths below -150m. The seismic-stratigraphic analysis of the Plio-Quaternary sequences is based on the stratigraphy defined by Juan et al., (2016). The sum of the plan curvature values was made with the help of ArcGis V10.2 using the focal statistics tool to smooth the noise at depths higher than 150m. (Fig. 5). The chronology 260 of the seismic stratigraphic boundaries was defined based on an age calibration on of data from scientific wells DSDP 121 and ODP 976, 977, 978, and 979 (FigFigs. 1 and 5) (Ercilla et al., 2016; Juan et al., 2016). Using the velocity analysis for the ODP well 976 (Soto et al., 2012), we considerassume an average P-wave velocity of 1750m/s for the Plio-Quaternary pelagic sedimentation.sediments. We propose seismic stratigraphy and sequential stratigraphy interpretations of depositional units 265 based on the nomenclature and general principles presented in the literature (Catuneanu, 2007; Catuneanu et al., 2011). -All seismic lines shown in the present manuscript are presented without interpretation uninterpreted in the supplementary materials (Figuresmaterial (Figs. S1 to S8, Supplementary materialsmaterial).

### 3. Results

#### 3.1. **Plio-Quaternary seismic stratigraphy**

- 270 The PlioPliocene-Quaternary sedimentary sequence of the southern margin of the south Alboran SeaMargin has been divided into three Pliocene (Pl1, Pl2, and Pl3) and four Ouaternary (Ot1 to Ot4) seismic units, based on the Juan et al. (2016) seismic stratigraphy (Fig. 5). These units are limited at the bottombase by discontinuity surfaces, M, PO, and P1 for the Pliocene units, and BQD, Q0 to Q2, for the Quaternary units. Boundaries represent These discontinuity surfaces are mostly defined by onlap and erosive surfaces; locally, downlap surfaces are identified (Fig. 6 and 7). Sub-parallel, parallel, oblique, and wavy stratified
- 275 reflections characterize the Plio-Quaternary Pliocene units. -Pl1, Pl2, and Pl3 units are pinching toward the structural highs and evidenceshow aggrading wedges wedge geometries. The Quaternary seismic units (QT1 to QT4) show an aggradational geometry and are confined to the foot of the folds where they pinch on the older tilted Pliocene deposits (Fig. 6 and 7)(Juan et al., 2016).
- Contouritic deposits and associated sedimentary features, MTDs and volcanic deposits constitute the PlioPliocene-Quaternary 280 unitsdeposits. The plastered driftsdrift type is dominant and contributes to cover the structural highs (Juan et al., 2016). In seismic reflection, truncations Truncations at the foot of topographic highs corresponds to contourite moats and channels on seismic lines (Fig. 7). Sediments presentshow local intercalations of lenticular chaotic or transparent facies that are interpreted as mass-flow deposits-and-corresponding to scars on the bathymetry (Fig. 3) (Rodriguez et al., 2017). Regarding the volcanic deposits, two buried volcanic edifices are identified on seismic reflection: the Big Al-Idrissi Volcano (FigFigs. 3-
- 285 8 and 11),8) and the Small Al-Idrissi Volcano (Fig.3, 6,9 and 119). Acoustically, they correspond to a seismic facies of poorly continuous, high-amplitude reflectors (Fig. 6, 8 and 9). Pliocene to Quaternary reflectors onlaps on onto these seismic unitsbodies (Fig. 8 and 9). They trend NE-SW following the trend of South Alboran Trough (Fig. 8 and 910).

The Big Al-Idrissi Volcano corresponds to a conic structure located to the North of the Ras Tarf (-Fig. 3, and 8) that has been interpreted as an N-S volcanic ridge in Bourgois et al. (1992). (Bourgois et al., 1992). The top of this seismic body merges with

- 290 the M-Reflector reflector (Fig. 8). Above, Plio-Quaternary seismic units showingbury this volcano and show prograding to aggrading sigmoid reflectors characterizes that characterize the growth of a continental shelf above the M reflector burying this volcano (Fig. 8). On the west side of this seamount, the trajectory of the offlap breaks is concave up, indicating that the rate of progradation decreases progressively with time. Reflectors onlaps terminations on the bottomsets and foresets of the prograding seismic units-mark, marking the beginning of a retrogradation after 1.81 Ma (Fig. 8). West--dipping normal faults
- 295

offset the depositional unit of prograding sigmoid reflectors (Fig. 8). These normal faults correspond to scarps at the seafloor (Fig. 8 and 11). Toward the top of the sequence, a unit of flat-lying reflectors corresponds to the bottomsets of the late-Pleistocene Moroccan shelf offshore of the Ras Tarf correspond to a unit of flat lying reflectors (Fig. (Fig. 8). The flat top of the Big Al-Idrissi volcano culminates at an approximate depth of 150-200 m below the present-day sea level and corresponds to a toplap surface (Fig. 8).

- 300 ItIn the South Alboran ThroughTrough, the Small Al-Idrissi volcano shows a roughly NNE SSW spatial extent and has a 4-5 km wide conic structure and trends roughly NNE-SSW (Fig. 9, 10 and 11). This seismic body intercalated within the Pl1 seismic unit pinches abruptly toward the West (Fig. 9). [This body corresponds to a rounded high at the seafloor (Fig. 11), which pinches abruptly toward the West (Fig. 911). The top of the Pl1 seismic unit rests unconformably on this seismic body indicating an early-Pliocene age (Fig. 9). In the Francesc Pagès Bank, a seismic body with similar facies is present at the core of an NNE-SSW striking anticline (Fig. 6), truncated by the M reflector (Fig. 6).
- The stratigraphic architecture of the shelf north<u>North</u> of the Nekor Basin<u>, the shelf</u> records an early-Quaternary regression (Fig. 12). We follow the Q1 surface northeastward toward the top of the submerged shelf surrounding the Big Al-Idrissi Volcano (Fig. 8). The Q0 reflector corresponds to an unconformity at the bottom of prograding oblique reflectors. This depositional unit displays the geometry of continental shelf deposits. The most distal offlap break shows the maximum extent
- of the <u>Pleistocene</u> continental shelf north of the Nekor Basin-during the Pleistocene. It indicates that the retrogradation of the shoreline starts before 1.12 Ma and after 1.81Ma (Q1 reflector, Fig. 12). The most distal offlap break near Al-Hoceima is located around 312±30 mstwt, (twt, two-way travel time), corresponding to a depth of 188±5 m below sea level (Fig. 12). In the distal part of the shelf, we interpret a seismic body of poorly continuous wavy reflectors deposited above an erosional surface as a local mass transport complex, which could mark an early Quaternary destabilization of the shelf.

#### 315 **3.2.** Evidence and style of the compressive deformation

The seismic stratigraphy shows that the Plio Quaternary sequence records two principal phases of deformation. Folds and faults along the Alboran Ridge demonstrate a Pliocene compressive phase. On the Moroccan shelf, the stratigraphic pattern indicates a regressive trend. The second phase is younger and corresponds to the developing activity of strike slip and normal faults, which control the local transgressions of the Moroccan shelf.

#### 320 <u>3.2. Tectonic structures</u>

#### 3.2.1. Folded structures of the South Alboran Ridge (SAR)

Bounded by the WAB and the South Alboran Trough, the SAR region corresponds to an N065° 80km long folded area (Fig. 6). The shortening in the SAR is distributed from east to west over thea 10 to 25 km wide SARfolding structure, composed of a series of two to four 4 km-wavelength anticlines (Figs. 6 and 10). Northward-verging anticlines characterize the northern
front of deformation front (Fig. 6). In the eastern part of the SAR, the Francesc Pagès and the Eurofleet Highs correspond to a south-verging 10 km wide antiformal stack of pinched anticlines, in a 10 km narrow fold, over south verging thrusts (MAB16 and 14; Fig. 6). Several southward and northward dipping blind thrusts affect the M reflector (Fig. 6). From East to West and above the thruststhrust faults, a series of anticlines and synclines draw a sigmoidal pattern (Fig. 10). Azimuths of the hinge axis tendlines trend toward the E Wa mean N085° direction at the center of the folds and toward an N065a N070° direction

330 toward the tips of the folds, therefore demonstrating left lateral deflections of their hinge axis and overall sigmoidal shape (Fig.

<del>6 and 10)...</del> The orientation of the most western tip of the SAR changes from NE-SW to E-W (Fig. 6). <u>The azimuths of the</u> <u>Pliocene folds in the southern termination of the NAR trend N058° (Fig. 10).</u>

Below the M surface, truncated Miocene seismic units show local folding (Fig. 6f)(Do Couto et al., 2016). It indicates that a shortening occurred in the SAR before the Messinian Salinity Crisis (MSC). The lateral and vertical strata pattern of the Plio-

- 335 Quaternary units shows that the shortening occurs mostly during the Pliocene.<u>6f</u>). Along the northern flank of the SAR, tectonic tilting and <u>P0 to BQD unconformities show</u> the growth of the contouritic drift deposits produce P0 to BQD unconformities during tectonic tilting (Fig. 7). The intra Pliocene unconformities, the tilting of the Pliocene units, and the aggradation of Quaternary contouritic deposits on top of the sedimentary sequence indicate a compressive deformation ending around the early Quaternary (Fig. 6 and 9).7). Within the Pliocene sequence, the folding appears to be progressive and diachronic from
- 340 East to West. At the foot of the Francesc Pagès Bank, P1 reflectors are unconformably lying on the P0 reflector (Fig. 7a). At the foot of the Ramon Margalef High, Pliocene reflectors older than P1 show a more even geometry with constant thickness, where thicknesses, and P0 is a conformable surface (Fig. 7b).

Parallel to the SAR, the South Alboran Trough corresponds to a syncline that narrows from East to West (Fig. 6). Its northern flank is steeper than the southern one (Fig. 6). The local <u>thickness</u> variations-of thicknesses reveal the non-cylindrical folding
of the syncline (Fig. 6 and 10). The progressive tilt of the QT1 to QT4 units and internal growth strata reveal a more continuous Quaternary to Pleistocene folding of the South Alboran Trough (Fig. 6, and 9) near the Al-Idrissi fault zone (Fig. 9). It indicates that local folding persists during the Quaternary.Figs. 6 and 9).

#### 3.2.2. The Al-Idrissi fault zone

- At present day, the AIF is ana NNE-SSW fault zone composed of several segments followingthat locally follow the older structuralNE-SW trend (Fig.-of the Alboran Ridge (Figs. 10 and 11). CrossingThe AIF forms a clear positive flower structure across the eastern end of the Francesc Pagès Bank and the western end of the NAR, it forms a positive flower structure distinct from the Pliocene thrust of the Alboran Ridge (Fig.- (Fig. 13). The flower structureAIF here corresponds to a left-lateral restraining bend-of the AIF, connecting the northern and southern segments. This structure partially reactivates NE-SW Pliocene thrusts of the Alboran Ridge and affects the most-recent Quaternary sediments (Fig. 11 and 13), whereas Pliocene thrusts appear to be abandoned during the Quaternary (Fig. 13). The depth of the Messinian unconformity at the western tip of the Alboran Ridge is lower than at the Francesc Pages Bank (Fig. 10), indicating different uplift/subsidence rates from either part of the AIF.). The location of the left-lateral restraining bend is highlighted at present-day by the cluster of compressive focal mechanisms (Fig. 4) (Stich et al., 2010). Locally some Pliocene thrusts appear to be abandoned during the Quaternary (Fig. 13). The Alboran Ridge than at the Francesc Pages Bank (Fig. 10), indicating different uplift/subsidence rates from either part of the AIF.). The location of the left-lateral restraining bend is highlighted at present-day by the cluster of compressive focal mechanisms (Fig. 4) (Stich et al., 2010). Locally some Pliocene thrusts appear to be abandoned during the Quaternary (Fig. 13).
  360 (Fig. 10), indicating differential uplift/subsidence across the AIF.
- At the southern tip of the AIF, NNE-SSW <u>active</u> fault segments affect present day deposits and correspond to splay faults distributing the deformation <u>that affect present-day deposits</u> (Fig. 9 and 11). At the seafloor, the fault traces are clear toward the southwest where they offset the Small Al-Idrissi volcano and link to the Bokoya fault (Fig. 10 and 11). Below the volcanic

facies, poor acoustic penetration prohibits the interpretation of tectonic structures (Fig. 9). At the seafloor, the fault tracks are

- 365 clear toward the southwest where they offset the Small Al Idrissi volcano and link to the Bokoya fault (Fig. 10 and 11). AffectingOn the SAR,north-dipping flank of the South Alboran Ridge, we observe N145° strikingtrending lineaments at the seafloor that correspond to sub-vertical normal faults affecting the sub-surface sediments (Fig. 11 and 14). At the northern flank of the SAR, the The fault network describes forms a 10-12km wide shear zone (Fig. 14). The recognition of pockmarks at the seafloor and signal attenuation near the faults on the seismic reflection data suggest fluid seepages along active faults
- 370 (Fig. 14) (e.g., Judd and Hovland, 2009). Northward, the faults disappear atbelow the seafloor under the present-day depositional part of the contourite. In the subsurface, they drift. These faults affect Q1 and Q2 surfaces demonstrating late-Pleistocene activity (Fig. 14b). Southward, we lost the fault trackstraces disappear against the hinge axis of the Francesc Pagès fold. At the southwestern flank of the Francesc Pagès fold, similarBank. Similar NW-SE striking faults affect the seafloor at the southwestern flank of the Francesc Pagès bank (Fig. 11a). These N145° lineaments observed at the surface-correspond to
- the normal faults pointed in red on the TOPAS profile (Fig. 6b),11b) that uplift the western block-of the fault wall. Despite reduced expression at the seafloor, this fault zone continues southeast, where it affects the whole Plio-Quaternary sequence (Fig. 9). Along the AIF, the vertical offset of the P1 surface is around 100m (Fig. 9). Between the N145° faults and the AIF, several fault segments affect the subsurface, highlighting the distributed deformation-that occurs between the N145° faults and the AIF with a higher apparent vertical offset along the AIF (Fig. 9).

#### **4. Discussion**

Our results show at least two phases of tectonic activity from the Early-Pliocene to the present day. <u>Based on a literature</u> <u>synthesis (Fig. 15)</u> and <u>our new data, we show</u> that the Al-Idrissi Fault zone is a <u>newyoung</u> feature (<1.8Ma) <u>that</u> profoundly <u>affecting theaffects</u> regional deformation. The first phase of <u>compressivetranspressive</u> deformation <u>startsstarted</u> probably during the Tortonian and ends during the early Quaternary, with the <u>possible</u>-local occurrence of volcanism-<u>and a strike slip</u> ecomponent. The second phase <u>starts</u> clearly <u>started</u> after 1.8 Ma and continues today. It corresponds to a <u>strike slip phase with</u> an important extensional component.transtensive tectonic regime. Both phases evidence the overall oblique convergence and <u>essential</u>-control <u>ofby</u> deep structures, which we detail thereafter.

#### 4.1. MioMiocene-Pliocene to Early Quaternary strain partitioning

The first tectonic phase occurred from the Mio Pliocene to the Early Quaternary. The overall geometry of the SAR deformation shows the development of imbricated folds distributed throughout a left lateral shear zone along N065° striking thrust faults (Fig. 6). Truncated folds (Fig. 6f) indicate that shortening started in the South Alboran Ridge before the Messinian Salinity Crisis (MSC) (Do Couto et al., 2016). The lateral and vertical stratal pattern of the Plio-Quaternary units shows that the shortening occurs mostly during the Pliocene. The overall geometry of deformation in the SAR shows the development of a N065° shear zone that partitioned the deformation in imbricated folds and thrusts and left-lateral shear (Fig. 6). The change of 395 stacking pattern of the Pliocene deposits along the folds suggests a diachronous growth during the Pliocene with the lateral variation of the uplift rates (Fig. 6 and 7). The <u>intra-Pliocene unconformities</u>, the tilting of the Pliocene units, and the aggradation of contourites at the foot of the SAR indicatesQuaternary contourite deposits indicate a relative quiescence of the folding during the Quaternary after 2.6 Ma (Juan et al., 2016).

Mio-The Pliocene deformation is locally contemporaneous of with volcanism. The lateral continuity of the highly reflective

- facies from west to east suggests that the Small Al Idrissi and the Big Al-Idrissi volcanoes are part of a volcanic structure that is offset by local extensional faults during the Pleistocene (Fig. 8 and 10). This highly reflective material triggers the acoustic masking of the reflections below (Fig. 9), as observed in debris-avalanche deposits elsewhere (Le Friant et al., 2002, 2009). The intercalation of this volcanic material toward the top of the Pl1 unit indicates thatdates the Small Al-Idrissi Volcano could be older thanbetween 4.5 Ma but younger than and 5.33 Ma (Fig. 9). The NE-SW distribution of the volcanic material suggests
- 405 a syn-folding infill of the N065° striking syncline axisof the South Alboran Trough (Fig. 10). The local volcanism can beis contemporaneous to the volcanic activity occurring to the Northnorth of the Alboran Ridge, dated between 6 and 4.5 Ma (Duggen et al., 2008). This volcanism generally shows high K content consistent with melting occurringoccurred above a thinned continental lithosphere (Duggen et al., 2008). It could also be the product of decompression partial melting after the Messinian Salinity Crisis, as proposed for the onshore Pliocene Moroccan volcano by Sternai et al., (2017). The observed The
- 410 local volcanism suggests that the SAR could have accommodated westward thinning of the crust in the WABWest Alboran Basin from late Miocene to Pliocene. This extension could be linked to the transition from slab rollback to delamination as proposed in Petit al<sub>11</sub> (2015).

The sigmoid folds in the SAR draw a rhombic pattern (Fig. 10). Within the N065° trend of the SAR, their overall E W strikes evidence left lateral transpression during the Pliocene. NE SW thrust faults distribute the deformation and probably

- 415 accommodate the strike slip motion during the Pliocene. The distribution of the deformation into left lateral motion and shortening reflects the onset of an oblique direction of shortening relatively from NE — SW basement faults (i.e., between the Nekor and Jebha Fault and the Alboran Ridge). The left lateral shear component of the deformation of the Alboran domain implies vertical axis rotation of the basement faults (Fig. 15a to 15c), as demonstrated elsewhere (Koyi et al., 2016; Tadayon et al., 2018). It suggests that the deformation progressively switches from left lateral transpressive to compressive strike slip
- 420 (Fig. 15a and 15b). Vertical axis rotations favor a progressive change from transpressive to more purely compressive. The development of oblique faults and thickness variation in the sedimentary cover, which results in non-cylindrical thrust wedges, lateral escape of frontal thrust sheets and vertical axis block rotations demonstrate the influence of a viscous layer at the base of the sedimentary covers, as demonstrated from analog modeling (Storti et al., 2007). In the SAR, such a weak layer can correspond to the early Miocene under compacted shales at the bottom of the sedimentary covers (Soto et al., 2008, 2012).
- 425 Such weak layer can explain why the deformation is distributed in the SAR, whereas it appears to be more localized in the NAR.

The Pliocene NE-SW thrust faults distribute the deformation between the Nekor and Jebha Fault and the Alboran Ridge and accommodate the strike-slip motion during the Pliocene. The angle between the N065° trend of the SAR and the N085° trend

of internal folds evidence a N-S maximum horizontal shortening direction in the SAR (in the present-day structural framework)

- 430 and indicates left-lateral transpression during the Pliocene folding. The 20° angle between left-lateral fault zone and shortening direction indicates pure-shear dominated transpression in the SAR (e.g., Fossen et al., 1994; Fossen and Tikoff, 1998). It reflects the oblique shortening direction relatively to the NE—SW basement faults during the Pliocene. In the SAR, the Pliocene folds show a left-lateral deflection of their hinge lines from the E-W to NE-SW, drawing an overall sigmoidal shape (Figs. 6 and 10). Comparison of the structures in the SAR with analogue models of fold-and-thrust belt (e.g., ter Borgh et al., 1994).
- 435 2011; Koyi et al., 2016; Storti et al., 2007), suggests reactivation of basement faults and vertical-axis rotation of the faults (Fig. 16a to 16c). The development of E-W faults and thickness variation in the sedimentary cover, resulting in non-cylindrical thrust wedges, lateral escape of frontal thrust sheets and vertical-axis block rotations demonstrate the influence of a viscous layer. In the SAR, such a weak layer corresponds to the early-Miocene under-compacted shales at the base of the sedimentary cover (Soto et al., 2008, 2012). Such weak layer can explain why the deformation is distributed in the SAR, whereas it appears
- 440 to be more localized in the NAR. As the direction of relative plate motion between Africa-Eurasia is approximatively constant since 6 Ma (DeMets et al., 2015), left-lateral transpression in the SAR in the present-day framework is unlikely. Instead, it suggest a progressive rotation of basement faults relatively to the regional shortening direction since the Pliocene and a progressive change from left-lateral transpressive to more purely compressive deformation (Fig. 16a and 16b). This model is in accordance with the bookshelf
- 445 model, which assumes 2–3°/Ma progressive vertical-axis rotation of basement faults since the Pliocene (Meghraoui and Pondrelli, 2013).

<u>The offshore Pliocene</u> oblique compression offshore-is equivalent to transpressive tectonictectonics in the Rif (Table 1).
 <u>Theonshore (Fig. 15)</u>, where the area between the Nekor fault and the Jebha Fault accommodate accommodates distributed deformation onshore, and a transpressive deformation is recorded offshore around the SAR (Fig. 15a16a). The passive infilling of paleo-rias indicates relatively low vertical motion (Romagny et al., 2014), (Fig. 15). After 3.8 Ma, a transition from

- compression to radial extension (Benmakhlouf et al., 2012) causes NE-SW normal faulting and tectonic tilting of the Moroccan margin (Fig. <u>15b)16b</u> (Romagny et al., 2014). Toward the south-east, the Nekor fault has acted as a transpressive fault zone accommodating the shortening (Ait Brahim et al., 2002; Aït Brahim and Chotin, 1990). The offshore extensional faults prolonging the Nekor fault arewere sealed offshore by Pliocene deposits and were inverted as blind thrust faults during the Plio-Quaternary (Watts et al., 1993). In the external Rif, in southwest<u>the southwestward</u> continuity of the Nekor Fault, field studies demonstrate NE-SW compression (Roldán et al., 2014). <u>InterpretationsInterpretation</u> of 2D seismic reflection lines indicates thick-skin tectonic from Tortonian-early Messinian to Pliocene times, causing the uplift of
  - intramountainousintra-mountainous basins around the Nekor fault (Fig. 15a)16a) (Capella et al., 2016).

#### 4.2. Quaternary to present-day strain partitioning

#### 460 **4.2.1.** Evidences Evidence of Quaternary tectonic subsidence

In contrast to the SAR region, in the NARSouth Alboran Ridge, the recorded uplift increases through time in the North Alboran Ridge until it reaches a maximum around 2.45 Ma, withrelated to the development of a clear pop-up structure (Martínez-García et al., 2017). It (Fig. 15). This contrast could be linked to the incipient activity of the AIF and suggests that the AIF progressively decouples the deformation between the NAR and the SAR from 2.6 – 2.45 Ma (Table 1Fig. 16). Before 1.8 Ma, basinward motion of the shelf along the Big – Al Idrissi volcano and the normal regressive geometry of the shelf wedges argue for progradation driven by sediment supply. It canmay indicate positive accommodation at the coastline (Catuneanu et al., 2011). In the overall regressive trend, syncline formation can create accommodation space.

After 1.8 Ma, the later Pleistocene transgression is linked to the normal faulting along N-S faults (Fig. 8 and 12). Including the onshore Trougout and Boudinar faults, we interpret the N-S fault network as an *en-echelon* right-stepping set of normal faults (Fig. 10 and 1516). Focal mechanism and microstructural studies demonstrate that this fault network is likely to be active with a normal and a sinistral component at present day (Fig. 4) (Poujol et al. 2014). The local stratigraphy recorded the start of the activity of this tectonic structure-during the Pleistocene. The depth of the Pleistocene offlap breaks and the geometry of the shelves indicate evident tectonic subsidence during the Pleistocene contemporaneous with the northward tilting of the margin (Ammar et al., 2007). The Moroccan shelf underwent a local transgression and flooding characterized by the building

475 of transgressive wedges on top of a-prograding clinoforms (Fig. 78 and 12). The retrogradation of the shoreline startsstarted between 1.8 Ma and 1.12 Ma inon the margins of the Nekor Basin and the Big Al-Idrissi volcano (Table 1Fig. 16). The depthsdepth of the offlap breaks areis significantly lower than the maximum depths reached by the sea-level falls at Gibraltar during the Quaternary (Fig. 68 and 712) (Rohling et al. 2014) and proves the tectonic subsidence.

## 4.2.2. Evolution and localization of the Al-Idrissi fault zone

480 The beginning of the transgression of the shelf around the Big Al-Idrissi volcano and the Nekor Basin is approximately synchronous ofto the last shortening event along the NARNorth Alboran Ridge (1.8 to 1.12 Ma)(Table 1) (Fig. 15). The AIF has progressively propagated southward, activating the N-S right-stepping normal fault linking fromtowards the AIF to Boudinar and Nekor Basins during the Quaternary (Fig. 15b). Since *ca*. 1.8 Ma 1.12 Ma, the(Fig. 16b). The transgression of the shelf of the Big Al-Idrissi volcano and the subsidence of the Nekor Basin indicated localization of the deformation on a releasing bend activating N-S faults. The restraining bend in the northern part of the AIF affect the seafloor and is activated indicate the localization of deformation on a releasing bend activating these N-S faults.

<u>The apparent small lateral offset and the localization of deformation on the left-lateral-during the recent seismic crisis (Buforn et al., 2017; Galindo-Zaldívar et al., 2015). In the eastern part of the SAR, N145° normal faults are active with an orientation similar to the N140° normal faults accommodating the late Pleistocene extension in the Nekor Basin (Fig.-10, 11 and 14)</u>
 (Lafosse et al., 2017). From the local direction of the maximum horizontal stress field and focal mechanisms (Fig. 2b and 4)

15

(Neres et al., 2016), the fault zone is transtensive with a right lateral motion. We can regard this fault zone as an antithetic or extensional structure accommodating the present day left lateral motion along the AIF, or extensional structures related to the southern fault tip in the horsetail splay (Fig. 15c). The apparent low lateral offset and the localization of the deformation on the strike slip Boussekkour-Bokova fault zone after 0.8 Ma suggest that the localization of the deformation along the AIF is a

- 495 recent feature (Fig. 15e15 and 16c) (Lafosse et al. 2017). In this context, the normal faults in the Nekor Basin are equivalent to antithetic faults within a horsetail splay, that connect to the Trougout Fault and the Nekor faults (Fig. 15b16b). Such structures groware probably through related to a mechanism of relay ramp, like the one proposed in other strike-slip contexts such as the Paleogene Bowey Basin (Peacock and Sanderson, 1995). It denotes a progressive localization of the deformation along the AIF and westward migration of the deformation as proposed in Lafosse et al., 2017 and Galindo-Zaldivar et al., 2018
- 500 (Fig. <u>15c).</u>16c).

The left-lateral restraining bend in the northern part of the AIF affects the seafloor and was active during the recent seismic crisis (Buforn et al., 2017; Galindo-Zaldívar et al., 2015). In the eastern part of the SAR, the N145° normal faults are active with an orientation similar to the N140° normal faults in the Nekor Basin (Fig. 10, 11 and 14) (Lafosse et al., 2017). The local direction of the maximum horizontal stress field and focal mechanisms (Fig. 2b and 4) (Neres et al., 2016), indicate that the

- 505 fault zone is transfersive with a right-lateral motion. This fault zone may act as the conjugate to the present-day left-lateral AIF, or be an extensional structure related to the southern fault tip in the horsetail splay (Fig. 16c).
  - The inception of the southern Al-Idrissi fault zone after 1.8Ma is coherent with similar ages found for the inception of strikeslip tectonics in the Diibouti Plateau area where the set of conjugated strike slip Al Idrissi and Averroes faults is dated around -1.1Ma (Fig. 1 and Table 1)(Estrada et al., 2018; Gràcia et al., 2019; Perea et al., 2018).to the north of the NAR where the
- 510 set of conjugated Al-Idrissi and Averroes strike-slip faults is dated around 1 - 1.1Ma (Figs. 1, 15 and 16) (Estrada et al., 2018; Gràcia et al., 2019; Perea et al., 2018). The AIF decouples the deformation in the SAR and the NAR and acts as a transfer fault accommodating that connects the shortening north of the Alboran Ridge (Estrada et al., 2018) and the Rifian extrusion along the Nekor fault. The localization of the deformation along the AIF could be controlled by a Miocene pre-existing structure, as proposed in Martínez-García et al., (2017). At a crustal-scale, geophysical studies show a ~20-30km crustal thickness variation
- 515 atin the Al Hoceima region (Diaz et al., 2016), which can contribute to the localization of the deformation. The contrasts of crustal thickness origin either incontrasts are a consequence of Miocene oblique collision (Booth-Rea et al., 2012), lower erustcrustal doming during the Miocene transtension (Le Pourhiet et al., 2014), or removal of lower crust-removal associated to delamination processes (Bezada et al., 2014; Petit et al., 2015). The localization of the deformation on crustal heterogeneity heterogeneities has been evidenced in numerical models, for example, in the cratonic lithosphere (Burov et al., 1998). Similarly, the localization of the AIF evidences the control of the crustal thicknesses thickness variations resulting from
- 520

slab roll back and delamination processes.

#### 4.3. Evolution of the southeastern limit of the **Betico-Rifian**<u>Alboran</u> tectonic domain

The late Miocene-early Pliocene period in the Rif Belt matches the uplift of the Miocene intramountainous intra-mountainous basin along the Nekor fault under a transpressional tectonic regime compression and left-lateral displacement (Fig. 15a16 and 525 table 116a)(Capella et al., 2016). The uplift of those basins corresponds to the change from thin-skin to thick-skin deformation in the external Rif during the inversion of the deep Mesozoic extensional structures (Capella et al., 2016; Martínez-García et al., 2017) and during the transpressive deformation in the Temsamane units (Fig. 1)(Booth Rea et al., 2012). It suggests. Our preferred tectonic scenario consists of a progressive mechanical coupling between the African Margin and the Alboran Domain, locking the Nekor fault in its eastern segment (Fig. 15). In the External Rif, 16). This scenario is supported by paleo-530 magnetic data evidence from the External Rif that indicate at least 2015° of counter-clockwise rotation since the upper Miocene (Crespo Blanc et al., 2016; Platt et al., 2003). Progressive vertical axis rotation associated with the shortening of the Alboran Basin decreases the left lateral shear, and increase the compressive deformation along the Alboran Ridge (Fig 15b). Eventually, the deformation has localized on the AIF during the early Quaternary decoupling the deformation between the NAR and the SAR with a developing transtensive mode from 1.81 Ma (Fig. 15c). It induces (Crespo-Blanc et al., 2016, and references 535 therein). Progressive vertical-axis rotation associated with the shortening of the Alboran Basin decreases the left lateral shear,

- and increases the compressive deformation along the Alboran Ridge (Fig 16b). Eventually, the deformation has localized on the AIF during the early Quaternary, decoupling the deformation between the NAR and the SAR with a developing transtensive regime since 1.81 Ma (Fig. 16c). This evolution induced a change of strain partitioning along the TASZ illustrated by the transition from a Pliocene left-lateral shearing and folding of the SAR to a transtensive Quaternary deformation localized on the AIF and the Nekor Basin (Fig. 15).
- Changes of tectonic style in the Alboran Basin have been related to changes in the direction of far field forces (Martínez-García et al., 2013). However, since 5 Ma, the direction of Africa Eurasia convergence remains16). Since 6 Ma, the relative direction of Africa-Eurasia convergence has remained constant (DeMets et al. 2015). In), with a NNE-SSW direction in an absolute reference frame, the direction of convergence between Africa and Eurasia is NNE SSW, producing 15km of
- 545 shortening since 8Ma (Spakman et al., 2018). From GPS measurements and from present day stress and strain modelling, the Alboran tectonic domain can be considered as undergoing a clockwise rotation of 1.17°/Ma (Palano et al., 2013, 2015). This value has the same order of magnitude to the domino model from Meghraoui and Pondrelli (2013) of a tectonic block undergoing a long term clockwise rotation of 2.24°/Ma to 3.9°/Ma. This prohibits changes in the direction of far-field forces as the cause for changes of tectonic style in the Alboran Basin as suggested by Martínez-García et al. (2013).
- 550 In the Alboran Basin, the TASZ must rotate as well to accommodate the convergence and block rotation (Fig. 15). It follows that during the Pliocene and a part of the Pleistocene, the direction of far field forces is oblique to principal fault planes of the Alboran ridge. Because of the vertical axis rotation, the obliquity decreases progressively, which leads to the present day more orthogonal compression along the NAR (Fig. 2b and 15)(Cunha et al., 2012; Neres et al., 2016) and the inversion of the Alboran Basin and the Algerian Margin (Derder et al., 2013; Hamai et al., 2015; Martínez García et al., 2017). Therefore, the evolution

555 of the deformation in the Alboran Ridge represents the expected evolution of transpressive structures under a constant shortening and indentation of the African lithosphere (Fig. 15). Block rotations and transpressive folds propagation followed by transtensive deformation during the inception of the AIF represent successive steps within the tectonic inversion of the Alboran Domain since 8Ma.

Conversely, delamination may occur in the Rif from 6 Ma to the present dayOther scenarios consider that delamination

- occurred in the Rif since 6 Ma, explaining the structural pattern and extension in the Nekor basin (Bezada et al., 2013; Petit et al., 2015). Extension in the Nekor Basin and strike-slip along the Al-Idrissi Fault since 1.8 1.12 Ma would then correspond to a reappraisal of mantle delamination. However, this process corresponds to a long-term convective removal of the African lithosphere (Petit et al., 2015). To explain the progressive tectonic reorganization during the Plio-Quaternary, we do not favor this last hypothesis because we do not observe an increase of <u>widespread</u> long\_wavelength, <u>widespread</u> (>100 km) subsidence, <u>that is</u> usually associated to convective thinning of the lithosphere in thermomechanical models (e.g., Le Pourhiet et al., 2006;
  - Valera et al., 2011)(e.g., Le Pourhiet et al., 2006; Valera et al., 2011).
     Recent papers (Heit et al., 2017; Mancilla et al., 2015; Sun and Bezada, 2020) suggest that a slab tear propagates from the Betic to the western tip of the Alboran Ridge, with 4-5 clusters of a lithospheric thinningnecking distributed from North to South below the WABWest Alboran Basin (Sun and Bezada, 2020). It is not clear how fast this slab tear propagates from the
- 570 Betic to the studied area, and how it controls the Plio Quaternary deformation. The timing is of primordial importance because thermomechanical models proposeIt is unclear how fast this slab tear propagates from the Betic to the study area, and how it controls the Plio-Quaternary deformation. Since 4 Ma, slow uplift and extension are recorded in the central Rif (Fig. 15) (Romagny et al., 2014) and might mark the inception of the lithospheric necking. Since 1.8 1.12 Ma, vertical motion are local though, and associated to the activity if the AIF. The timing is of primordial importance as demonstrated by
- 575 thermomechanical models. These models show that slab detachment is a fast process that can occur in less than 1 Ma, causing a high amplitude topographic response (Duretz et al., 2011, 2012). Slow uplift and extension recorded in the central Rif (Table 1)(Romagny et al., 2014) could mark the inception of the lithospheric necking from 4 Ma. However, this hypothesis is still speculative because we do not observe radical changes in vertical motions in the WAB or in the study area. It indicates that the vertical pull due to the sinking lithosphere must be constant during the Plio Quaternary. Since 1.8 1.12 Ma, dip slips
- 580 faults along the AIF corresponds to a restraining bend and a horsetail splay and explain local vertical motions. It indicates that the vertical pull due to the sinking lithosphere must be constant during the Plio-Quaternary. It suggests that the necking of the sinking lithosphere is a slow process, or is very recent with yet indiscernible effects on the shallower structures in the upper plate.

In this framework, normal strike slip behaviour observed to the north of the NAR (Fig. 1)(Giaconia et al., 2015; Gràcia et al.,

585 2012; Grevemeyer et al., 2015; Palomino et al., 2011) goes a step further in the sense of an indentation of the Africa plate into the Alboran tectonic domain (Fig. 2)In this framework, normal strike-slip faulting observed to the north of the NAR (Fig. 1) (Estrada et al., 2018; Giaconia et al., 2015; Gràcia et al., 2012; Grevemeyer et al., 2015) provides an additional evidence of indentation by the Africa plate into the Alboran tectonic domain (Estrada et al., 2018; Palano et al., 2015). This indentation is accommodated through the left-lateral AIF and the right-lateral Averroes Yusuf fault zone (Fig. 1 and 1516) in a similar way

590 than the Palomares fault zone transferring the orthogonal shortening of the Iberian margin toward the Carboneras fault zone and the Central Alboran Sea (Estrada et al., 2018; Giaconia et al., 2015). In the SAR and the Nekor Basin, the present-day deformation under the transtensional regime (NNW-SSE to N-S extensional network and NNE-SSW strike-slip faults; Fig. 4 and 1516) is limited to the east by the Al-Idrissi fault. The deformation in the NAR is on the contrary clearly compressive (Estrada et al., 2018; Martínez-García et al., 2017) and the geodetic data indicates indicate similar displacements in the EAB 595 and in the Rifian units east of the Boudinar Basin (Koulali et al., 2011; Vernant et al., 2010). Such difference of behavior

suggests that the AIF may represent the present-day plate boundary between Africa and Alboran Domain.

#### Conclusion 5.

This study focuses focused on the tectonic evolution of the southern margin of the Alboran Sea during the Plio-Quaternary period, and particularly the distinct structural evolutions and interactions of the AIF and the ARAlboran Ridge, and the 600 mechanisms associated to their formation. The analysis of the seismic stratigraphy and the comparison between onshore and offshore tectonic structures leadsled to the following tectonic framework:

- (1) The TASZTrans Alboran Shear Zone, and in particular the Alboran Ridge, localized the deformation between the Miocene and the early Quaternary. Its orientation favors a strike-slip movement during its oblique shortening. The rhombic folded structures of the SAR illustrate a South Alboran Ridge underwent significant left-lateral displacement during the Pliocene. Consequently, during the Pliocene, the SAR accommodates the strain partitioning between left lateral strike slip and shortening.
- (2) Under the indentation of African lithosphere, vertical-axis block rotations, which lead led to a progressive compression on the Alboran Ridge and a voungerPleistocene activation under left lateral transtension along of the AIF.Al-Idrissi Fault. The subsidence of both the Nekor Basin and the Big Al-Idrissi volcano demonstratemarks the start of the transfersive deformation between 1.8 Ma and 1.12.
- (3) The SAR undergoes transpression whereas further east tectonic inversion of the Algerian and Iberian margin occurs. The area between the SARSouth Alboran Ridge and the Nekor fault is being progressively extruded southwestward, whereas east of the Al-Idrissi fault, the African lithosphere indents the Alboran tectonic domain. The AIFAI-Idrissi Fault transfers this indentation to the Nekor Basin, which accommodates the present day westward extrusion of the Rif and represents an incipient plate boundary since 1.8 Ma.
- Our findings demonstrate that at the scale of athe basin, strike-slip shear zones evolve in response to far-field forces but also in response to the local evolution of the Al-Idrissi Fault zone. This evolution is fast and achieved in less than 2 Ma and might be related to lithospheric necking below the WABWest Alboran Basin or mantle delamination below the Rif. In our opinion, the indentation of the African lithosphere into the Alboran tectonic domain explains better the scale and timing of the 620 deformation in the AIF.Al-Idrissi Fault. Additional modeling could be made help to hierarchize-better understand the different

605

610

615

19

processes, and further researches are. Further research is needed to better understand better what drives the timing and the evolution of such large scale-strike slip structures.

#### 6. Author contribution

Manfred Lafosse wrote the paper and conducted the study.

Elia d'Acremont and Christian Gorini leadled the oceanic surveys MARLBORO-1, 2 and SARAS. They contributed to the study and to the redaction of the present paper.

Alain Rabaute contributed to the data acquisition and processing, and to the redaction of the present paper.

-Jeroen Smit contributed to the redaction of the present paper.

Ferran Estrada contributed to the data acquisition and processing.

- Martin Jollivet-Castelot contributed to the stratigraphic interpretation.
   Juan Tomas Vazquez contributed to the data acquisition and processing.
   Jesus Galindo-Zaldivar and Gemma Ercilla contributed to the data acquisition and processing. They are the PI of the INCRISIS survey. Gemma Ercilla also contributed to the stratigraphic correlations and interpretations.
   Belen Alonso contributed to the stratigraphic correlations and interpretations.
- 635 Abdellah Ammar contributed to the data acquisition.

#### 7. Acknowledgement

We thank the members of the SARAS and Marlboro cruises in 2011 and 2012. We also thank Dr. Lodolo and Prof Déverchère, Dr Booth-Rea for their helpful comments and discussion. We also thank the editor, Dr Frederico Rossetti, for the attention provided to this manuscript. This work was funded by the French program Actions Marges, the EUROFLEETS program (FP7/2007-2013; n°228344), project FICTS-2011-03-01. The French program ANR- 17-CE03-0004 also supported this work. Seismic reflection data were processed using the Seismic UNIX SU and Geovecteur software. The processed seismic data were interpreted using Kingdom IHS Suite©software. This work also benefited from the Fauces Project (Ref CTM2015-65461-C2-R; MINCIU/FEDER) financed by "Ministerio de Economía y Competitividad y al Fondo Europeo de Desarrollo Regional" (FEDER).

#### 645 **8.** Competing interests

640

"The authors declare that they have no conflict of interest."

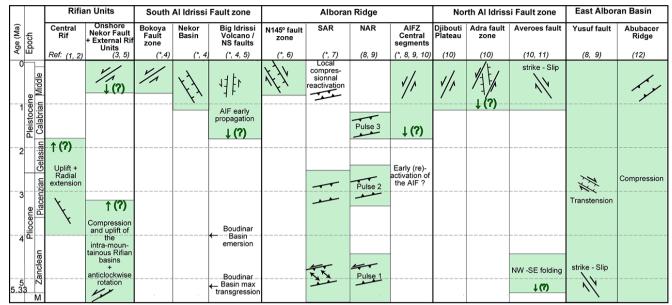


 Table 1.-Synthesis of the tectonic events in the Alboran Basin, and the Rif from the literature and the present study. \*, this study;

 650
 (1), Benmakhlouf et al., (2012) ; (2), Romagny et al., (2014) ; (3) Aït Brahim and Chotin, (1990), (4), Lafosse et al., (2017); (5),

 Azdimousa et al., (2006); (6), Calindo Zaldivar et al., (2018); (7) Juan et al., (2016); (8) Martínez-Carcía et al., (2013) ; (9), Martínez-García et al., (2017); (10), Gràcia et al., (2019); (11), Perca et al., (2018); (12) Giaconia et al., (2015). The main tectonic events are in green. Green arrows and question marks figure the age uncertainties of the main tectonic events.

#### **10.9.** Bibliography

665

d'Acremont, E., Gutscher, M.-A., Rabaute, A., Mercier de Lépinay, B., Lafosse, M., Poort, J., Ammar, A., Tahayt, A., Le Roy, P., Smit, J., Do Couto, D., Cancouët, R., Prunier, C., Ercilla, G. and Gorini, C.: High-resolution imagery of active faulting offshore Al Hoceima, Northern Morocco, Tectonophysics, doi:10.1016/j.tecto.2014.06.008, 2014.

Aït Brahim, L. and Chotin, P.: Oriental Moroccan Neogene volcanism and strike-slip faulting, Journal of African Earth Sciences, 11(3/4), 273–280, doi:https://doi.org/10.1016/0899-5362(90)90005-Y, 1990.

660 Ait Brahim, L., Chotin, P., Hinaj, S., Abdelouafi, A., El Adraoui, A., Nakcha, C., Dhont, D., Charroud, M., Sossey Alaoui, F., Amrhar, M., Bouaza, A., Tabyaoui, H. and Chaouni, A.: Paleostress evolution in the Moroccan African margin from Triassic to Present, Tectonophysics, 357(1–4), 187–205, doi:10.1016/S0040-1951(02)00368-2, 2002.

Alvarez-Marrón, J. and others: Pliocene to Holocene structure of the eastern Alboran Sea (western Mediterranean), in Proceedings of the Ocean Drilling Program-Scientific Results, vol. 161, pp. 345–355. [online] Available from: http://digital.csic.es/handle/10261/17611 (Accessed 19 June 2014), 1999.

Ammar, A., Mauffret, A., Gorini, C. and Jabour, H.: The tectonic structure of the Alboran Margin of Morocco, Revista de la Sociedad Geológica de España, 20(3–4), 247–271, 2007.

Ballesteros, M., Rivera, J., Muñoz, A., Muñoz-Martín, A., Acosta, J., Carbó, A. and Uchupi, E.: Alboran Basin, southern Spain—Part II: Neogene tectonic implications for the orogenic float model, Marine and Petroleum Geology, 25(1), 75–101, doi:10.1016/j.marpetgeo.2007.05.004, 2008.

670

685

700

Benmakhlouf, M., Galindo-Zaldívar, J., Chalouan, A., Sanz de Galdeano, C., Ahmamou, M. and López-Garrido, A. C.: Inversion of transfer faults: The Jebha–Chrafate fault (Rif, Morocco), Journal of African Earth Sciences, 73–74, 33–43, doi:10.1016/j.jafrearsci.2012.07.003, 2012.

Bezada, M. J., Humphreys, E. D., Toomey, D. R., Harnafi, M., Dávila, J. M. and Gallart, J.: Evidence for slab rollback in
 westernmost Mediterranean from improved upper mantle imaging, Earth and Planetary Science Letters, 368, 51–60,
 doi:10.1016/j.epsl.2013.02.024, 2013.

Bezada, M. J., Humphreys, E. D., Davila, J. M., Carbonell, R., Harnafi, M., Palomeras, I. and Levander, A.: Piecewise delamination of Moroccan lithosphere from beneath the Atlas Mountains, Geochemistry, Geophysics, Geosystems, 15(4), 975–985, doi:10.1002/2013GC005059, 2014.

680 Bezzeghoud, M. and Buforn, E.: Source parameters of the 1992 Melilla (Spain, MW= 4.8), 1994 Alhoceima (Morocco, MW= 5.8), and 1994 Mascara (Algeria, MW= 5.7) earthquakes and seismotectonic implications, Bulletin of the Seismological Society of America, 89(2), 359–372, 1999.

Biggs, J., Bergman, E., Emmerson, B., Funning, G. J., Jackson, J., Parsons, B. and Wright, T. J.: Fault identification for buried strike-slip earthquakes using InSAR: The 1994 and 2004 Al Hoceima, Morocco earthquakes, Geophysical Journal International, 166(3), 1347–1362, doi:10.1111/j.1365-246X.2006.03071.x, 2006.

Bird, P.: An updated digital model of plate boundaries, Geochem. Geophys. Geosyst., 4, 1027, doi:10.1029/2001gc000252, 2003.

Booth-Rea, G., Ranero, C., Martinez-Martinez, J.M., Grevemeyer and I.: Crustal types and Tertiary tectonic evolution of the Alboran sea, western Mediterranean, Geochem. Geophys. Geosyst., 8, Q10005, 2007.

690 Booth-Rea, G., Jabaloy-Sánchez, A., Azdimousa, A., Asebriy, L., Vílchez, M. V. and Martínez-Martínez, J. M.: Upper-crustal extension during oblique collision: the Temsamane extensional detachment (eastern Rif, Morocco): The Temsamane extensional detachment (eastern Rif, Morocco), Terra Nova, 24(6), 505–512, doi:10.1111/j.1365-3121.2012.01089.x, 2012.

ter Borgh, M. M., Oldenhuis, R., Biermann, C., Smit, J. H. W. and Sokoutis, D.: The effects of basement ramps on deformation of the Prebetics (Spain): A combined field and analogue modelling study, Tectonophysics, 502(1), 62–74, doi:10.1016/j.tecto.2010.04.013, 2011.

Bourgois, J., Mauffret, A., Ammar, A. and Demnati, A.: Multichannel seismic data imaging of inversion tectonics of the Alboran Ridge (Western Mediterranean Sea), Geo-Marine Letters, 12(2–3), 117–122, 1992.

Buforn, E., Pro, C., Sanz de Galdeano, C., Cantavella, J. V., Cesca, S., Caldeira, B., Udías, A. and Mattesini, M.: The 2016 south Alboran earthquake (M w = 6.4): A reactivation of the Ibero-Maghrebian region?, Tectonophysics, 712–713, 704–715, doi:10.1016/j.tecto.2017.06.033, 2017.

Burov, E., Jaupart, C. and Mareschal, J. C.: Large-scale crustal heterogeneities and lithospheric strength in cratons, Earth and Planetary Science Letters, 164(1–2), 205–219, doi:10.1016/S0012-821X(98)00205-2, 1998.

Calvert, A., Gomez, F., Seber, D., Barazangi, M., Jabour, N., Ibenbrahim, A. and Demnati, A.: An integrated geophysical investigation of recent seismicity in the Al-Hoceima region of North Morocco, Bulletin of the Seismological Society of America, 87(3), 637–651, 1997.

Calvert, A., Sandvol, E., Seber, D., Barazangi, M., Roecker, S., Mourabit, T., Vidal, F., Alguacil, G. and Jabour, N.: Geodynamic evolution of the lithosphere and upper mantle beneath the Alboran region of the western Mediterranean: Constraints from travel time tomography, J. Geophys. Res., 105(B5), 10871–10898, doi:10.1029/2000JB900024, 2000.

Capella, W., Matenco, L., Dmitrieva, E., Roest, W. M. J., Hessels, S., Hssain, M., Chakor-Alami, A., Sierro, F. J. and 710 Krijgsman, W.: Thick-skinned tectonics closing the Rifian Corridor, Tectonophysics, doi:10.1016/j.tecto.2016.09.028, 2016.

Catuneanu, O.: Principles of sequence stratigraphy, 1. ed., reprinted., Elsevier, Amsterdam., 2007.

705

725

Catuneanu, O., Galloway, W. E., Kendall, C. G. St. C., Miall, A. D., Posamentier, H. W., Strasser, A. and Tucker, M. E.: Sequence Stratigraphy: Methodology and Nomenclature, Newsletters on Stratigraphy, 44(3), 173–245, doi:10.1127/0078-0421/2011/0011, 2011.

715 Chalouan, A., Saji, R., Michard, A., Bally and W., A.: Neogene tectonic evolution of the southwestern Alboran basin as inferred from seismic data off Morocco, Aapg Bulletin-American Association of Petroleum Geologists, 81, 1161–1184, 1997.

Chalouan, A., Michard, A., El Kadiri, K., Negro, F., Frizon de Lamotte, D., Soto, J. I. and Saddiqi, O.: The Rif Belt, in Continental evolution: the geology of Morocco, pp. 203–302., 2008.

Comas, M. C., Platt, J. P., Soto, J. I. and Watts, A. B.: The origin and Tectonic History of the Alboran Basin: Insights from Leg 161 Results, Proceedings of the Ocean Drilling Program Scientific Results, 161, 555–580, 1999.

Crespo-Blanc, A., Comas, M. and Balanyá, J. C.: Clues for a Tortonian reconstruction of the Gibraltar Arc: Structural pattern, deformation diachronism and block rotations, Tectonophysics, doi:10.1016/j.tecto.2016.05.045, 2016.

Cunha, T. A., Matias, L. M., Terrinha, P., Negredo, A. M., Rosas, F., Fernandes, R. M. S. and Pinheiro, L. M.: Neotectonics of the SW Iberia margin, Gulf of Cadiz and Alboran Sea: a reassessment including recent structural, seismic and geodetic data: Neotectonics SW Iberia Gulf of Cadiz Alboran, Geophysical Journal International, 188(3), 850–872, doi:10.1111/j.1365-246X.2011.05328.x, 2012.

- Custódio, S., Lima, V., Vales, D., Cesca, S. and Carrilho, F.: Imaging active faulting in a region of distributed deformation from the joint clustering of focal mechanisms and hypocentres: Application to the Azores–western Mediterranean region, Tectonophysics, 676, 70–89, doi:10.1016/j.tecto.2016.03.013, 2016.
- 730 DeMets, C., Iaffaldano, G. and Merkouriev, S.: High-resolution Neogene and Quaternary estimates of Nubia-Eurasia-North America Plate motion, Geophys. J. Int., 203(1), 416–427, doi:10.1093/gji/ggv277, 2015.

Derder, M. E. M., Henry, B., Maouche, S., Bayou, B., Amenna, M., Besse, J., Bessedik, M., Belhai, D. and Ayache, M.: Transpressive tectonics along a major E-W crustal structure on the Algerian continental margin: Blocks rotations revealed by a paleomagnetic analysis, Tectonophysics, 593, 183–192, doi:10.1016/j.tecto.2013.03.007, 2013.

735 Díaz, J., Gil, A., Carbonell, R., Gallart, J. and Harnafi, M.: Constraining the crustal root geometry beneath Northern Morocco, Tectonophysics, 689, 14–24, doi:10.1016/j.tecto.2015.12.009, 2016.

Diaz, J., Gallart, J. and Carbonell, R.: Moho topography beneath the Iberian-Western Mediterranean region mapped from controlled-source and natural seismicity surveys, Tectonophysics, 692, 74–85, doi:10.1016/j.tecto.2016.08.023, 2016.

Dillon, W. P., Robb, J. M., Greene, H. G. and Lucena, J. C.: Evolution of the continental margin of southern Spain and the 740 Alboran Sea, Marine Geology, 36(3), 205–226, doi:10.1016/0025-3227(80)90087-0, 1980.

Do Couto, D.: Evolution géodynamique de la mer d'Alboran par l'étude des bassin sédimentaires, Université Pierre et Marie Curie, Paris, FRANCE, 16 January., 2014.

Do Couto, D., Gumiaux, C., Augier, R., Lebret, N., Folcher, N., Jouannic, G., Jolivet, L., Suc, J.-P. and Gorini, C.: Tectonic inversion of an asymmetric graben: Insights from a combined field and gravity survey in the Sorbas basin, Tectonics, 33(7), 745 2013TC003458, doi:10.1002/2013TC003458, 2014.

Do Couto, D., Gorini, C., Jolivet, L., Lebret, N., Augier, R., Gumiaux, C., d'Acremont, E., Ammar, A., Jabour, H. and Auxietre, J.-L.: Tectonic and stratigraphic evolution of the Western Alboran Sea Basin in the last 25 Myrs, Tectonophysics, 677–678, 280-311, doi:10.1016/j.tecto.2016.03.020, 2016.

Duggen, S., Hoernle, K., van den Bogaard, P. and Harris, C.: Magmatic evolution of the Alboran region: The role of subduction 750 in forming the western Mediterranean and causing the Messinian Salinity Crisis, Earth and Planetary Science Letters, 218(1-2), 91–108, doi:10.1016/S0012-821X(03)00632-0, 2004.

Duggen, S., Hoernle, K., Klügel, A., Geldmacher, J., Thirlwall, M., Hauff, F., Lowry, D. and Oates, N.: Geochemical zonation of the Miocene Alborán Basin volcanism (westernmost Mediterranean): geodynamic implications, Contributions to Mineralogy and Petrology, 156(5), 577–593, doi:10.1007/s00410-008-0302-4, 2008.

755 Duretz, T., Gerya, T. V. and May, D. A.: Numerical modelling of spontaneous slab breakoff and subsequent topographic response, Tectonophysics, 502(1–2), 244–256, doi:10.1016/j.tecto.2010.05.024, 2011.

Duretz, T., Schmalholz, S. M. and Gerva, T. V.: Dynamics of slab detachment, Geochemistry, Geophysics, Geosystems, 13(3), doi:10.1029/2011GC004024, 2012.

Dziewonski, A. M., Chou, T.-A. and Woodhouse, J. H.: Determination of earthquake source parameters from waveform data 760 for studies of global and regional seismicity, J. Geophys. Res., 86(B4), 2825–2852, doi:10.1029/JB086iB04p02825, 1981.

Ekström, G., Nettles, M. and Dziewoński, A. M.: The global CMT project 2004–2010: Centroid-moment tensors for 13,017 earthquakes, Physics of the Earth and Planetary Interiors, 200–201, 1–9, doi:10.1016/j.pepi.2012.04.002, 2012.

El Alami, S. O., Tadili, B. A., Cherkaoui, T. E., Medina, F., Ramdani, M., Brahim, L. A. and Harnafi, M.: The Al Hoceima earthquake of May 26, 1994 and its aftershocks: a seismotectonic study, ANALI DI GEOFISICA, 41(4), 519–537, 1998.

El Azzouzi, M., Bellon, H., Coutelle, A. and Réhault, J.-P.: Miocene magmatism and tectonics within the Peri-Alboran orogen 765 (western Mediterranean), Journal of Geodynamics, 77, 171–185, doi:10.1016/j.jog.2014.02.006, 2014.

Ercilla, G., Juan, C., Hernández-Molina, F. J., Bruno, M., Estrada, F., Alonso, B., Casas, D., Farran, M., Llave, E., García, M., Vázquez, J. T., D'Acremont, E., Gorini, C., Palomino, D., Valencia, J., El Moumni, B. and Ammar, A.: Significance of bottom currents in deep-sea morphodynamics: An example from the Alboran Sea. Marine Geology,

770 doi:10.1016/j.margeo.2015.09.007, 2016.

> Estrada, F., Ercilla, G., Gorini, C., Alonso, B., Vázquez, J. T., García-Castellanos, D., Juan, C., Maldonado, A., Ammar, A. and Elabbassi, M.: Impact of pulsed Atlantic water inflow into the Alboran Basin at the time of the Zanclean flooding, Geo-Marine Letters, 31(5–6), 361–376, doi:10.1007/s00367-011-0249-8, 2011.

Estrada, F., Vazquez, J. T., Ercilla, G., Alonso, B., d'Acremont, E., Gorini, C., Gomez, M., Fernandez-Puga, M. C., Ammar,
A. and El Moumni, B.: Recent tectonic inversion of the Central Alboran Zone, Resúmenes de la 2<sup>a</sup> Reunión Ibérica sobre Fallas Activas y Paleosismología, 51, 2014.

Estrada, F., Galindo-Zaldívar, J., Vázquez, Gemma, E., D'Acremont, E., Belén, B. and Gorini, C.: Tectonic indentation in the central Alboran Sea (westernmost Mediterranean), Terra Nova, 30(1), 24–33, doi:10.1111/ter.12304, 2018.

Faccenna, C., Becker, T.W., Lucente, F.P., Jolivet, L., Rossetti and F.: History of subduction and back-arc extension in the Central Mediterranean, Geophys. J. Int., 145, 1–21, 2001.

Fossen, H. and Tikoff, B.: Extended models of transpression and transtension, and application to tectonic settings, Geological Society, London, Special Publications, 135(1), 15–33, doi:https://doi.org/10.1144/GSL.SP.1998.135.01.02, 1998.

Fossen, H., Tikoff, B. and Teyssier, C.: Strain modeling of transpressional and transtensional deformation, Norsk Geologisk Tidsskrift, 74(3), 134–145, 1994.

785 Galindo-Zaldívar, J., González-Lodeiro, F. and Jabaloy, A.: Stress and palaeostress in the Betic-Rif cordilleras (Miocene to the present), Tectonophysics, 227(1–4), 105–126, doi:10.1016/0040-1951(93)90090-7, 1993.

790

Galindo-Zaldívar, J., Azzouz, O., Chalouan, A., Pedrera, A., Ruano, P., Ruiz-Constán, A., Sanz de Galdeano, C., Marín-Lechado, C., López-Garrido, A., Anahnah, F. and Benmakhlouf, M.: Extensional tectonics, graben development and fault terminations in the eastern Rif (Bokoya–Ras Afraou area), Tectonophysics, 663, 140–149, doi:10.1016/j.tecto.2015.08.029, 2015.

Galindo-Zaldivar, J., Ercilla, G., Estrada, F., Catalán, M., d'Acremont, E., Azzouz, O., Casas, D., Chourak, M., Vazquez, J. T., Chalouan, A., Galdeano, C. S. de, Benmakhlouf, M., Gorini, C., Alonso, B., Palomino, D., Rengel, J. A. and Gil, A. J.: Imaging the Growth of Recent Faults: The Case of 2016–2017 Seismic Sequence Sea Bottom Deformation in the Alboran Sea (Western Mediterranean), Tectonics, 0(0), doi:10.1029/2017TC004941, 2018.

795 Garcia-Castellanos, D., Villasenor and A.: Messinian salinity crisis regulated by competing tectonics and erosion at the Gibraltar arc, Nature, 480, 359–363, 2011.

Gensous, B., Tesson, M. and Winnock, E.: La marge meridionale de la mer d'alboran: caracteres structuro-sedimentaires et evolution recente, Marine Geology, 72, 341–370, doi:10.1016/0025-3227(86)90127-1, 1986.

Giaconia, F., Booth-Rea, G., Ranero, C. R., Gràcia, E., Bartolome, R., Calahorrano, A., Lo Iacono, C., Vendrell, M. G.,
Cameselle, A. L., Costa, S., Gómez de la Peña, L., Martínez-Loriente, S., Perea, H. and Viñas, M.: Compressional tectonic inversion of the Algero-Balearic basin: Latemost Miocene to present oblique convergence at the Palomares margin (Western Mediterranean), Tectonics, 34(7), 2015TC003861, doi:10.1002/2015TC003861, 2015.

Gill, R. C. O., Aparicio, A., El Azzouzi, M., Hernandez, J., Thirlwall, M. F., Bourgois, J. and Marriner, G. F.: Depleted arc volcanism in the Alboran Sea and shoshonitic volcanism in Morocco: geochemical and isotopic constraints on Neogene tectonic processes, Lithos, 78(4), 363–388, doi:10.1016/j.lithos.2004.07.002, 2004.

Gràcia, E., Pallàs, R., Soto, J. I., Comas, M., Moreno, X., Masana, E., Santanach, P., Diez, S., García, M. and Dañobeitia, J.: Active faulting offshore SE Spain (Alboran Sea): Implications for earthquake hazard assessment in the Southern Iberian Margin, Earth and Planetary Science Letters, 241(3–4), 734–749, doi:10.1016/j.epsl.2005.11.009, 2006.

Gràcia, E., Bartolome, R., Lo Iacono, C., Moreno, X., Stich, D., Martínez-Diaz, J. J., Bozzano, G., Martínez-Loriente, S., 810 Perea, H., Diez, S., Masana, E., Dañobeitia, J. J., Tello, O., Sanz, J. L., Carreño, E. and EVENT-SHELF Team: Acoustic and seismic imaging of the Adra Fault (NE Alboran Sea): in search of the source of the 1910 Adra earthquake, Nat. Hazards Earth Syst. Sci., 12(11), 3255–3267, doi:10.5194/nhess-12-3255-2012, 2012.

Gràcia, E., Grevemeyer, I., Bartolomé, R., Perea, H., Martínez-Loriente, S., Gómez de la Peña, L., Villaseñor, A., Klinger, Y., Lo Iacono, C., Diez, S., Calahorrano, A., Camafort, M., Costa, S., d'Acremont, E., Rabaute, A. and Ranero, C. R.: Earthquake crisis unveils the growth of an incipient continental fault system, Nature Communications, 10(1), doi:10.1038/s41467-019-11064-5, 2019.

815

830

Grevemeyer, I., Gràcia, E., Villaseñor, A., Leuchters, W. and Watts, A. B.: Seismicity and active tectonics in the Alboran Sea, Western Mediterranean: Constraints from an offshore-onshore seismological network and swath bathymetry data, J. Geophys. Res. Solid Earth, 120(12), 2015JB012073, doi:10.1002/2015JB012073, 2015.

820 Hamai, L., Petit, C., Abtout, A., Yelles Chaouche, A. and Déverchère, J.: Flexural behaviour of the north Algerian margin and tectonic implications, Geophys. J. Int., 201(3), 1426–1436, doi:10.1093/gji/ggv098, 2015.

Gutscher, M.-A., Malod, J., Rehault, J.-P., Contrucci, I., Klingelhoefer, F., Mendes-Victor, L. and Spakman, W.: Evidence for<br/>active subduction beneath Gibraltar, Geology, 30(12), 1071–1074, doi:10.1130/0091-<br/>7613(2002)030<1071:EFASBG>2.0.CO;2, 2002.

825 Hatzfeld, D., Caillot, V., Cherkaoui, T.-E., Jebli, H. and Medina: Microearthquake seismicity and fault plane solutions around the Nékor strike-slip fault, Morocco, Earth and Planetary Science Letters, 120(1–2), 31–41, doi:https://doi.org/10.1016/0012-821X(93)90021-Z, 1993.

Heit, B., Mancilla, F. de L., Yuan, X., Morales, J., Stich, D., Martín, R. and Molina-Aguilera, A.: Tearing of the mantle lithosphere along the intermediate-depth seismicity zone beneath the Gibraltar Arc: The onset of lithospheric delamination, Geophysical Research Letters, 44(9), 4027–4035, doi:10.1002/2017GL073358, 2017.

Jolivet, L. and Faccenna, C.: Mediterranean extension and the Africa-Eurasia collision, Tectonics, 19(6), 1095–1106, doi:10.1029/2000TC900018, 2000.

Jolivet, L., Augier, R., Faccenna, C., Negro, F., Rimmele, G., Agard, P., Robin, C., Rossetti, F. and Crespo-Blanc, A.: Subduction, convergence and the mode of backarc extension in the Mediterranean region, Bulletin de la Société Géologique de France, 179(6), 525–550, doi:https://doi.org/10.2113/gssgfbull.179.6.525, 2008.

Jolivet, L., Faccenna, C. and Piromallo, C.: From mantle to crust: Stretching the Mediterranean, Earth and Planetary Science Letters, 285(1–2), 198–209, doi:10.1016/j.epsl.2009.06.017, 2009.

Juan, C., Ercilla, G., Javier Hernández-Molina, F., Estrada, F., Alonso, B., Casas, D., García, M., Farran, M., Llave, E., Palomino, D., Vázquez, J.-T., Medialdea, T., Gorini, C., D'Acremont, E., El Moumni, B. and Ammar, A.: Seismic evidence of current-controlled sedimentation in the Alboran Sea during the Pliocene and Quaternary: Palaeoceanographic implications, Marine Geology, doi:10.1016/j.margeo.2016.01.006, 2016.

Judd, A. and Hovland, M.: Seabed Fluid Flow: The Impact on Geology, Biology and the Marine Environment, Cambridge University Press., 2009.

Koulali, A., Ouazar, D., Tahayt, A., King, R. W., Vernant, P., Reilinger, R. E., McClusky, S., Mourabit, T., Davila, J. M. and
 Amraoui, N.: New GPS constraints on active deformation along the Africa–Iberia plate boundary, Earth and Planetary Science
 Letters, 308(1–2), 211–217, doi:10.1016/j.epsl.2011.05.048, 2011.

Koyi, H., Nilfouroushan, F. and Hessami, K.: Modelling role of basement block rotation and strike-slip faulting on structural pattern in cover units of fold-and-thrust belts, Geological Magazine, 153(5–6), 827–844, doi:10.1017/S0016756816000595, 2016.

850 Lafosse, M., d'Acremont, E., Rabaute, A., Mercier de Lépinay, B., Tahayt, A., Ammar, A. and Gorini, C.: Evidence of quaternary transtensional tectonics in the Nekor basin (NE Morocco), Basin Res, 29(4), 470–489, doi:10.1111/bre.12185, 2017.

Le Pourhiet, L., M. Gurnis and Saleeby, J.: Mantle instability beneath the Sierra Nevada Mountains in California and Death Valley extension, Earth and Planetary Science Letters, 251(1–2), 104–119, doi:10.1016/j.epsl.2006.08.028, 2006.

855 Le Friant, A., Boudon, G., Komorowski, J.-C. and Deplus, C.: L'île de la Dominique, à l'origine des avalanches de débris les plus volumineuses de l'arc des Petites Antilles, Comptes Rendus Geoscience, 334(4), 235–243, doi:https://doi.org/10.1016/S1631-0713(02)01742-X, 2002.

Le Friant, A., Boudon, G., Arnulf, A. and Robertson, R. E. A.: Debris avalanche deposits offshore St. Vincent (West Indies): Impact of flank-collapse events on the morphological evolution of the island, Journal of Volcanology and Geothermal Research, 179(1–2), 1–10, doi:10.1016/j.jvolgeores.2008.09.022, 2009.

860

875

Le Pourhiet, L., Huet, B. and Traoré, N.: Links between long-term and short-term rheology of the lithosphere: Insights from strike-slip fault modelling, Tectonophysics, 631, 146–159, doi:10.1016/j.tecto.2014.06.034, 2014.

Leblanc, D. and Olivier, P.: Role of strike-slip faults in the Betic-Rifian orogeny, Tectonophysics, 101(3–4), 345–355, doi:10.1016/0040-1951(84)90120-3, 1984.

865 Lisiecki, L. E. and Raymo, M. E.: A Pliocene-Pleistocene stack of 57 globally distributed benthic δ18O records, Paleoceanography, 20(1), PA1003, doi:10.1029/2004PA001071, 2005.

Mancilla, F. de L., Booth-Rea, G., Stich, D., Pérez-Peña, J. V., Morales, J., Azañón, J. M., Martin, R. and Giaconia, F.: Slab rupture and delamination under the Betics and Rif constrained from receiver functions, Tectonophysics, 663, 225–237, doi:10.1016/j.tecto.2015.06.028, 2015.

870 Martínez-Díaz, J. J. and Hernández-Enrile, J. L.: Neotectonics and morphotectonics of the southern Almería region (Betic Cordillera-Spain) kinematic implications, Int J Earth Sci (Geol Rundsch), 93(2), 189–206, doi:10.1007/s00531-003-0379-y, 2004.

Martínez-García, P., Soto, J. I. and Comas, M.: Recent structures in the Alboran Ridge and Yusuf fault zones based on swath bathymetry and sub-bottom profiling: evidence of active tectonics, Geo-Marine Letters, 31(1), 19–36, doi:10.1007/s00367-010-0212-0, 2011.

Martínez-García, P., Comas, M., Soto, J. I., Lonergan, L. and Watts, A. B.: Strike-slip tectonics and basin inversion in the Western Mediterranean: the Post-Messinian evolution of the Alboran Sea, Basin Research, 25(4), 361–387, doi:10.1111/bre.12005, 2013.

Martínez-García, P., Comas, M., Lonergan, L. and Watts, A. B.: From extension to shortening: tectonic inversion distributed
 in time and space in the Alboran Sea, Western Mediterranean: Tectonic inversion in the Alboran Sea, Tectonics, doi:10.1002/2017TC004489, 2017.

Medina, F. and Cherkaoui, T.-E.: The South-Western Alboran Earthquake Sequence of January-March 2016 and Its Associated Coulomb Stress Changes, Open Journal of Earthquake Research, 6(01), 35, 2017.

Meghraoui, M. and Pondrelli, S.: Active faulting and transpression tectonics along the plate boundary in North Africa, Ann. 685 Geophys., 55(5), doi:10.4401/ag-4970, 2013.

Muñoz, A., Ballesteros, M., Montoya, I., Rivera, J., Acosta, J. and Uchupi, E.: Alborán Basin, southern Spain—Part I: Geomorphology, Marine and Petroleum Geology, 25(1), 59–73, doi:10.1016/j.marpetgeo.2007.05.003, 2008.

Neres, M., Carafa, M. M. C., Fernandes, R. M. S., Matias, L., Duarte, J. C., Barba, S. and Terrinha, P.: Lithospheric deformation in the Africa-Iberia plate boundary: Improved neotectonic modeling testing a basal-driven Alboran plate, J. Geophys. Res. Solid Earth, 121(9), 2016JB013012, doi:10.1002/2016JB013012, 2016.

Nocquet, J.-M.: Present-day kinematics of the Mediterranean: A comprehensive overview of GPS results, Tectonophysics, 579, 220–242, doi:10.1016/j.tecto.2012.03.037, 2012.

Nocquet, J.-M. and Calais, E.: Geodetic Measurements of Crustal Deformation in the Western Mediterranean and Europe, Pure and Applied Geophysics, 161(3), 661–681, doi:10.1007/s00024-003-2468-z, 2004.

895 Nur, A., Ron, H. and Scotti, O.: Fault mechanics and the kinematics of block rotations, Geology, 14(9), 746-749, doi:10.1130/0091-7613(1986)14<746:FMATKO>2.0.CO;2, 1986.

Palano, M., González, P. J. and Fernández, J.: Strain and stress fields along the Gibraltar Orogenic Arc: Constraints on active geodynamics, Gondwana Research, 23(3), 1071–1088, doi:10.1016/j.gr.2012.05.021, 2013.

Palano, M., González, P. J. and Fernández, J.: The Diffuse Plate boundary of Nubia and Iberia in the Western Mediterranean:
 Crustal deformation evidence for viscous coupling and fragmented lithosphere, Earth and Planetary Science Letters, 430, 439–447, doi:10.1016/j.epsl.2015.08.040, 2015.

Palomino, D., Vázquez, J. T., Ercilla, G., Alonso, B., López González, N. and Díaz del Río, V.: Interaction between seabed morphology and water masses around the seamounts on the Motril Marginal Plateau (Alboran Sea, Western Mediterranean), Geo Mar Lett, 31(5–6), 465–479, doi:10.1007/s00367-011-0246-y, 2011.

905 Paulatto, M., Watts, A. B. and Peirce, C.: Potential field and high-resolution bathymetry investigation of the Monowai volcanic centre, Kermadec Arc: implications for caldera formation and volcanic evolution, Geophys. J. Int., ggt512, doi:10.1093/gji/ggt512, 2014.

Peacock, D. C. P. and Sanderson, D. J.: Strike-slip relay ramps, Journal of structural geology, 17(10), 1351–1360, doi:10.1016/0191-8141(95)97303-W, 1995.

910 Peña, L. G. de la, Ranero, C. R. and Gràcia, E.: The Crustal Domains of the Alboran Basin (Western Mediterranean), Tectonics, 37(10), 3352–3377, doi:10.1029/2017TC004946, 2018.

Perea, H., Gràcia, E., Martínez-Loriente, S., Bartolome, R., de la Peña, L. G., de Mol, B., Moreno, X., Iacono, C. L., Diez, S., Tello, O., Gómez-Ballesteros, M. and Dañobeitia, J. J.: Kinematic analysis of secondary faults within a distributed shear-zone reveals fault linkage and increased seismic hazard, Marine Geology, 399, 23–33, doi:10.1016/j.margeo.2018.02.002, 2018.

915 Perouse, E., Vernant, P., Chery, J., Reilinger, R. and McClusky, S.: Active surface deformation and sub-lithospheric processes in the western Mediterranean constrained by numerical models, Geology, 38(9), 823–826, doi:10.1130/G30963.1, 2010.

Petit, C., Pourhiet, L. L., Scalabrino, B., Corsini, M., Bonnin, M. and Romagny, A.: Crustal structure and gravity anomalies beneath the Rif, northern Morocco: implications for the current tectonics of the Alboran region, Geophys. J. Int., 202(1), 640–652, doi:10.1093/gji/ggv169, 2015.

920 Platt, J.P., Allerton, S., Kirker, A.I., Mandeville, C., Mayfield, A., Platzman, E., Rimi and A.: The ultimate arc: Differential displacement, oroclinal bending, and vertical axis rotation in the External Betic Rif arc, Tectonics, 22, 1017, 2003.

Reicherter, K. R. and Reiss, S.: The Carboneras Fault Zone (southeastern Spain) revisited with Ground Penetrating Radar-Quaternary structural styles from high-resolution images, Geologie en Mijnbouw, 80(3/4), 129–138, 2001.

Roberts, A.: Curvature attributes and their application to 3 D interpreted horizons, First break, 19(2), 85-100, 2001.

925 Rodriguez, M., Maleuvre, C., Jollivet-Castelot, M., d'Acremont, E., Rabaute, A., Lafosse, M., Ercilla, G., Vázquez, J.-T., Alonso, B. and Ammar, A.: Tsunamigenic submarine landslides along the Xauen–Tofiño banks in the Alboran Sea (Western Mediterranean Sea), Geophysical Journal International, 209(1), 266–281, doi:https://doi.org/10.1093/gji/ggx028, 2017.

930

935

Roldán, F. J., Galindo-Zaldívar, J., Ruano, P., Chalouan, A., Pedrera, A., Ahmamou, M., Ruiz-Constán, A., Sanz de Galdeano, C., Benmakhlouf, M., López-Garrido, A. C., Anahnah, F. and González-Castillo, L.: Basin evolution associated to curved thrusts: The Prerif Ridges in the Volubilis area (Rif Cordillera, Morocco), Journal of Geodynamics, 77, 56–69, doi:10.1016/j.jog.2013.11.001, 2014.

Romagny, A., Ph. Münch, Cornée, J.-J., Corsini, M., Azdimousa, A., Melinte-Dobrinescu, M. C., Drinia, H., Bonno, M., Arnaud, N., Monié, P., Quillévéré, F. and Ben Moussa, A.: Late Miocene to present-day exhumation and uplift of the Internal Zone of the Rif chain: Insights from low temperature thermochronometry and basin analysis, Journal of Geodynamics, 77, 39–55, doi:10.1016/j.jog.2014.01.006, 2014.

Ron, H., Beroza, G. and Nur, A.: Simple model explains complex faulting, Eos Trans. AGU, 82(10), 125-129, doi:10.1029/EO082i010p00125-01, 2001.

Ruiz-Constán, A., Galindo-Zaldívar, J., Pedrera, A., Célérier, B., Marín-Lechado and C.: Stress distribution at the transition from subduction to continental collision (northwestern and central Betic Cordillera), Geochem. Geophys. Geosyst., 12, 940 Q12002, doi:10.1029/2011gc003824, 2011.

Scholz, C. H., Ando, R. and Shaw, B. E.: The mechanics of first order splay faulting: The strike slip case, Journal of Structural Geology, 32(1), 118–126, doi:10.1016/j.jsg.2009.10.007, 2010.

Soto, I., J., Fernandez-Ibanez, Fermin, Talukder, Asrar, Martinez-Garcia, Pedro and Anonymous: Miocene shale tectonics in the Alboran Sea (western Mediterranean), Abstracts with Programs - Geological Society of America, 40, 187, 2008.

945 Soto, J. I., Fernández-Ibáñez, F. and Talukder, A. R.: Recent shale tectonics and basin evolution of the NW Alboran Sea, The Leading Edge, 31(7), 768–775, doi:https://doi.org/10.1190/tle31070768.1, 2012.

Spakman, W., Chertova, M. V., van den Berg, Arie. and van Hinsbergen, D. J. J.: Puzzling features of western Mediterranean tectonics explained by slab dragging, Nature Geoscience, doi:10.1038/s41561-018-0066-z, 2018.

Sternai, P., Caricchi, L., Garcia Castellanos, D., Jolivet, L., Sheldrake, T. E. and Castelltort, S.: Magmatic pulse driven by sea level changes associated with the Messinian salinity crisis, Nature Geoscience, 10(10), 783–787, doi:10.1038/ngeo3032, 2017.

Stich, D., Mancilla, F. d. L., Baumont, D. and Morales, J.: Source analysis of the Mw 6.3 2004 Al Hoceima earthquake (Morocco) using regional apparent source time functions, Journal of Geophysical Research, 110(B6), doi:10.1029/2004JB003366, 2005.

Stich, D., Serpelloni, E., de Lis Mancilla, F. d. L. and Morales, J.: Kinematics of the Iberia–Maghreb plate contact from seismic moment tensors and GPS observations, Tectonophysics, 426(3–4), 295–317, doi:10.1016/j.tecto.2006.08.004, 2006. Stich, D., Martín, R. and Morales, J.: Moment tensor inversion for Iberia–Maghreb earthquakes 2005–2008, Tectonophysics, 483(3–4), 390–398, doi:10.1016/j.tecto.2009.11.006, 2010.

Storti, F., Soto Marin, R., Rossetti, F. and Casas Sainz, A. M.: Evolution of experimental thrust wedges accreted from alongstrike tapered, silicone-floored multilayers, Journal of the Geological Society, 164(1), 73–85, doi:10.1144/0016-76492005-186, 2007.

Sun, M. and Bezada, M.: Seismogenic Necking During Slab Detachment: Evidence From Relocation of Intermediate-Depth Seismicity in the Alboran Slab, Journal of Geophysical Research: Solid Earth, 125(2), e2019JB017896, doi:10.1029/2019JB017896, 2020.

960

Tadayon, M., Rossetti, F., Zattin, M., Calzolari, G., Nozaem, R., Salvini, F., Faccenna, C. and Khodabakhshi, P.: The long term evolution of the Doruneh Fault region (Central Iran): A key to understanding the spatio temporal tectonic evolution in the hinterland of the Zagros convergence zone, edited by C. Frassi, Geological Journal, doi:10.1002/gj.3241, 2018.

Tesson, M., Gensous, B. and Lambraimi, M.: Seismic analysis of the southern margin of the Alboran Sea, Journal of African Earth Sciences (1983), 6(6), 813–821, doi:10.1016/0899-5362(87)90038-8, 1987.

Thurner, S., Palomeras, I., Levander, A., Carbonell, R. and Lee, C.-T.: Ongoing lithospheric removal in the western
 Mediterranean: Evidence from Ps receiver functions and thermobarometry of Neogene basalts (PICASSO project),
 Geochemistry, Geophysics, Geosystems, 15(4), 1113–1127, doi:10.1002/2013GC005124, 2014.

Valera, L., J., Negredo, M., A., Jiménez-Munt and I.: Deep and near-surface consequences of root removal by asymmetric continental delamination, Tectonophysics, 502, 257–265, doi:10.1016/j.tecto.2010.04.002, 2011.

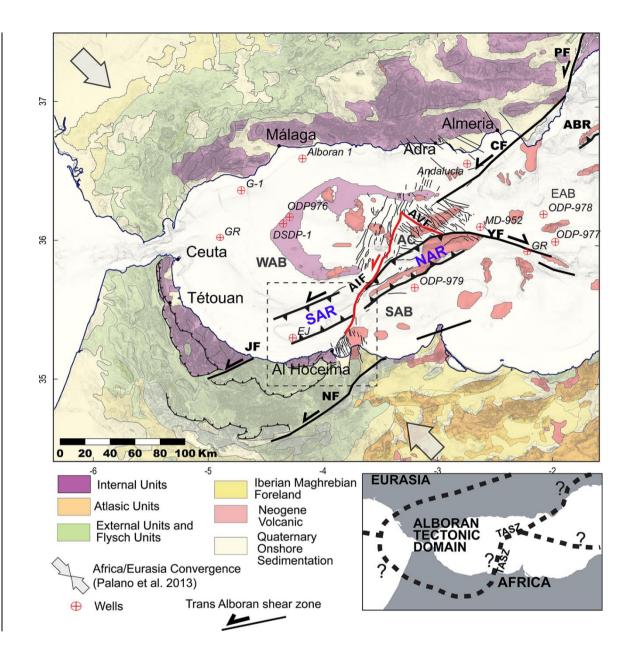
Van der Woerd, J., Dorbath, C., Ousadou, F., Dorbath, L., Delouis, B., Jacques, E., Tapponnier, P., Hahou, Y., Menzhi, M.,
 Frogneux, M. and Haessler, H.: The Al Hoceima Mw 6.4 earthquake of 24 February 2004 and its aftershocks sequence, Journal of Geodynamics, 77, 89–109, doi:10.1016/j.jog.2013.12.004, 2014.

Vázquez, J. T., Estrada, F., Vegas, R., Ercilla, G., d'Acremont, E., Fernández-Salas, L. M. and Alonso, B.: Quaternary tectonics influence on the Adra continental slope morphology (northern Alboran Sea), 2014.

 Vernant, P., Fadil, A., Mourabit, T., Ouazar, D., Koulali, A., Davila, J. M., Garate, J., McClusky, S. and Reilinger, R.: Geodetic
 constraints on active tectonics of the Western Mediterranean: Implications for the kinematics and dynamics of the Nubia-Eurasia plate boundary zone, Journal of Geodynamics, 49(3–4), 123–129, doi:10.1016/j.jog.2009.10.007, 2010.

Watts, A. B., Platt, J. P. and Buhl, P.: Tectonic evolution of the Alboran Sea basin, Basin Research, 5(3), 153–177, doi:https://doi.org/10.1111/j.1365-2117.1993.tb00063.x, 1993.

**<u>11.10.</u>** Figures



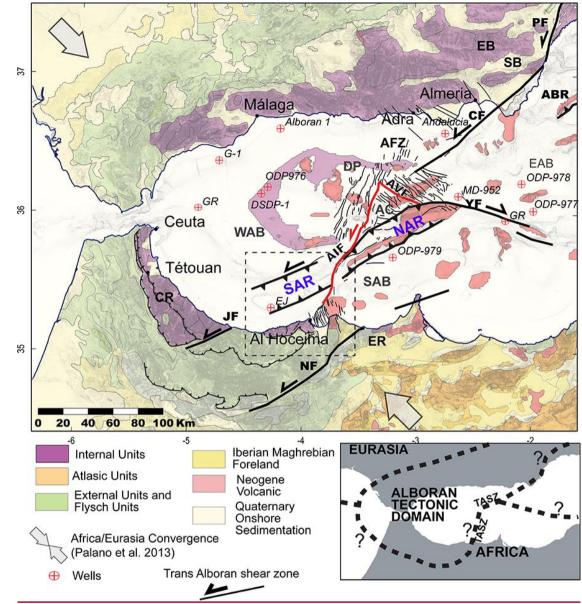


Figure 1. Topographic map and principal structural units of the Alboran region. Structural units in the studied area modified from Chalouan et al., (2008); Comas et al., (1999); Leblanc and Olivier, (1984); Romagny et al., (2014). The Trans Alboran Shear Zone 990 (TASZ) indicates the motion inferred for the Late-Miocene - Pliocene period. The red faults are the present-day active Al-Idrissi fault and its conjugated Averroes Fault. AC, Alboran Channel; AFZ, Adra Fault Zone; AVR, Averroes Fault; ABR, Abubacer Ridge; CF, Carboneras Fault; CR, Central Rif; DJ Djibouti Plateau; EB, Eastern Betic; EAB; East Alboran Basin; AIF, Al-Idrissi Fault; ER, Eastern Rif; JF, Jebha fault; NF, Nekor Fault; SAB, South Alboran Basin; SAR, South Alboran Ridge; SB, Sorbas Basin; NAR, North Alboran Ridge; -YF, Yusuf Fault; WAB, West Alboran Basin. Inset: Hypotheses of plate boundaries between an Alboran tectonic domain and the African plate from Nocquet, (2012).

995

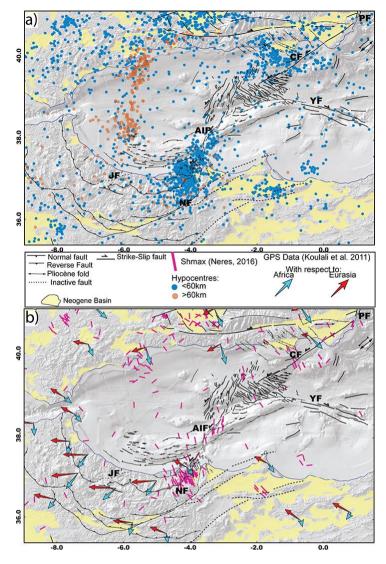
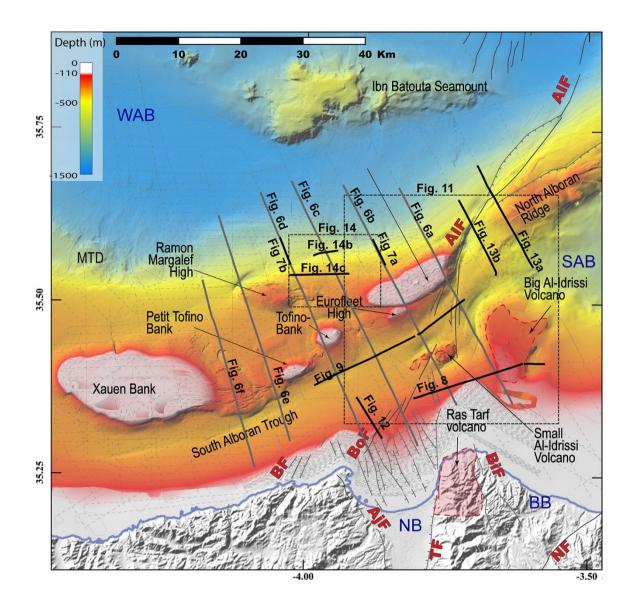


Figure 2. Maps showing the distribution of the seismicity along the Neogene tectonic structures in the Alboran Sea. a) Neotectonic map of the Alboran region modified from d'Acremont et al., (2014), -Alvarez-Marrón and others, (1999), Chalouan et al., (1997), Estrada et al., (2014), Gràcia et al., (2006), (2012); Lafosse et al., (2016), Martínez-García et al., (2011), Muñoz et al., (2008), Perea et al., (2014)Perea et al., (2014); Vázquez et al., (2014) and from this study. Seismicity from IGN catalogue 1970-2017 (http://www.ign.es/), only earthquakes with Mw >= 3 and depth >=2 km are figured. b) GPS data from Koulali et al., (2011) and Sh<sub>max</sub> from Neres et al., (2016). See figure 1 for scale. CF, Carboneras fault; PF, Palomares fault; YF, Yusuf fault; NF, Nekor fault; AIF, Al-Idrissi fault zone.



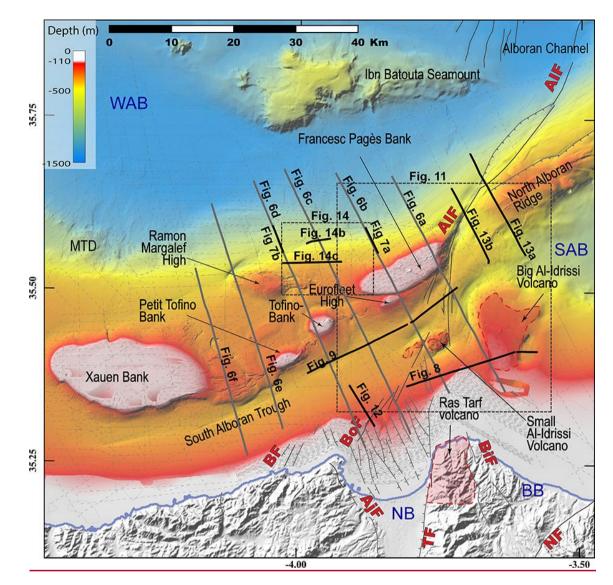
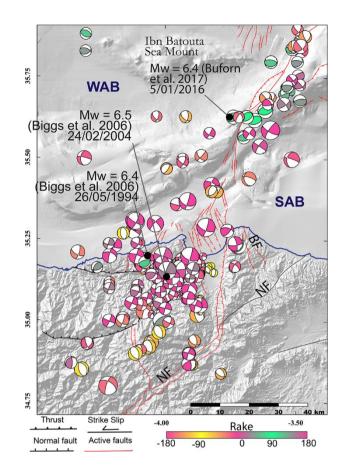


Figure 3. Bathymetry of the studied area showing the main morpho-structural features of the studied area. Dark grey and black lines, positions of the seismic lines used in the study. MTD, Mass Transport Deposits; WAB, West Alboran Basin; SAB, South
 Alboran Basin; BB, Boudinar Basin; BF: Boussekkour Fault; Bof, Bokoya Fault; BiF, Boudinar Fault; NB, Nekor Basin; NF, Nekor Fault; AIF; Al-Idrissi Fault zone; TF, Trougout fault; AjF, Adjir-Imzouren Fault.



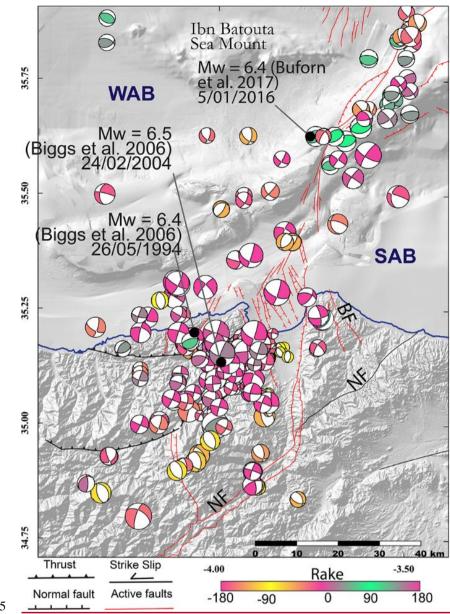
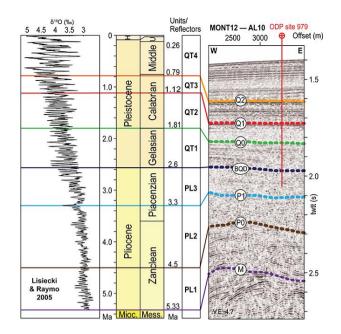
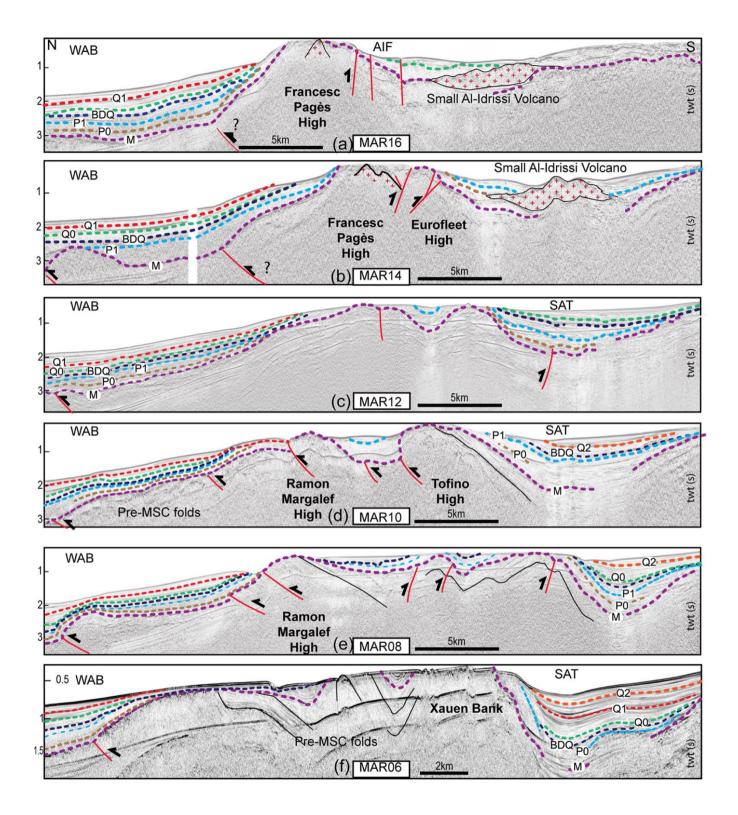


Figure 4. Map of the distribution of the present-day deformation showing strike-slip and compressive deformation along the northern part of the studied area and extensional and strike-slip structures along the southern part.- Focal mechanism till 2014 period from the compilation of Custódio et al.(2016) and for the year 2016 from GCMT project (http://www.globalcmt.org/; Dziewonski et al., 1981; Ekström et al., 2012). The size of the focal mechanisms corresponds to the magnitude values (from Mw= 2.3 to 6.4). Structural data compiled from Ballesteros et al., (2008); Biggs et al., (2006); Buforn et al., (2017); Chalouan et al., (1997);

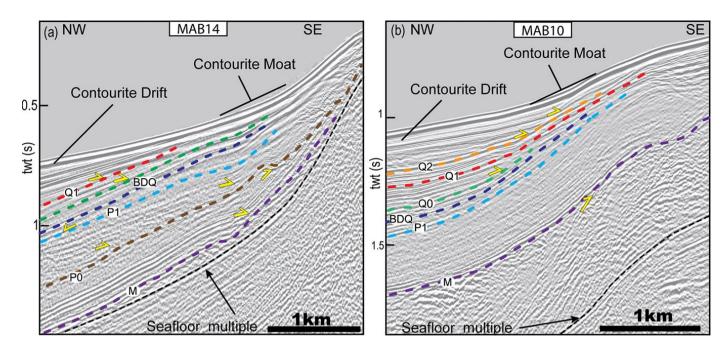
1020 to 6.4). Structural data compiled from Ballesteros et al., (2008); Biggs et al., (2006); Buforn et al., (2017); Chalouan et al., (1997); Lafosse et al., (2017) and Martínez-García et al., (2011). BF, Boudinar Fault, WAB, West Alboran Basin; SAB, South Alboran Basin; NF, Nekor fault.



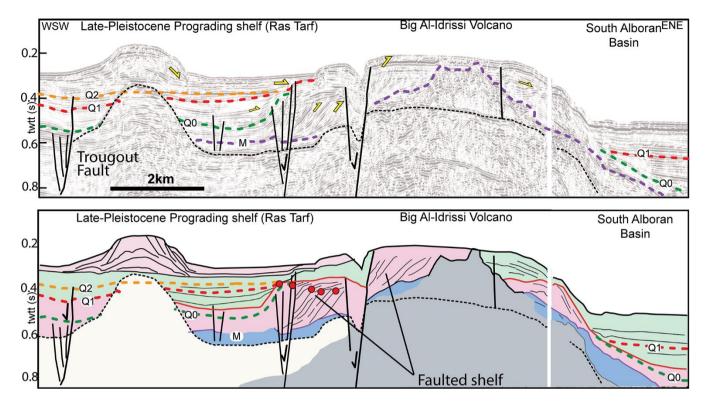
1025 Figure 5. Well log correlation to the seismic section, seismic line crossing the location of the ODP 979 site, vertical stacking of the Pliocene and Quaternary units, and available  $\delta^{18}$ O curve from Lisiecki and Raymo (2005). The colors of the stratigraphic surfaces are the same as in the following seismic lines.



1030 Figure 6. Multichannel seismic lines showing the Plio-Quaternary stratigraphy and structural features. Dashed and colored lines are the stratigraphic surface defined in figure 5. Black reflectors, pre-MSC reflectors. The seismic section (a) to (f) are ordered from east to west. WAB, South Alboran Basin; SAT, South Alboran Trough; AIF, Al-Idrissi Fault zone.



1035 Figure 7: Seismic unconformities at the foot slope of the northern flank of the South Alboran Ridge. a) Seismic line at the foot of the Francesc Pagès bank. b) Seismic line at the foot of the Ramon Margalef high. The seismic lines show the diachronism of the deformation affecting the SAR during the Pliocene. After 2.6 Ma, the moats of the contourites pinch at the feet of the folds.



- 1040 Figure 8: Multichannel seismic profile showing the transgression of marine sediment (in green) over the prograding shelf to the edges of the Big Al-Idrissi volcano (in pink) crossing the Ras Tarf Promontory and the Big Al-Idrissi Volcano. Dashed black reflector, multiple of the seafloor. Red points, offlap break (Paleo-shore line) marking the concave up trajectories of the offlap breaks and progradation of the shelf and the first transgression before 1.81Ma. The red surface is a maximum regressive surface in the sense of Catuneanu et al. (2011). The seismic line shows the transgression of marine sediment (in green) over the Pliocene to Quaternary
- 1045 prograding shelf to the edges of the Big Al-Idrissi volcano (in pink). Older depositional units are colored in blue and the acoustic basement in grey.

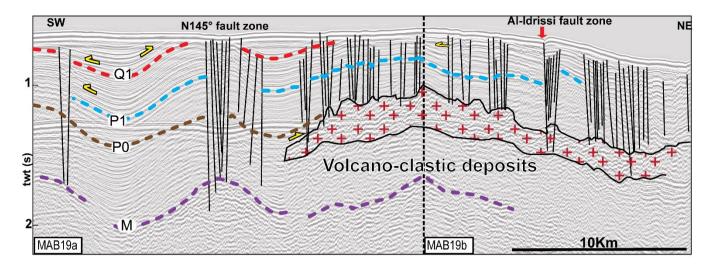
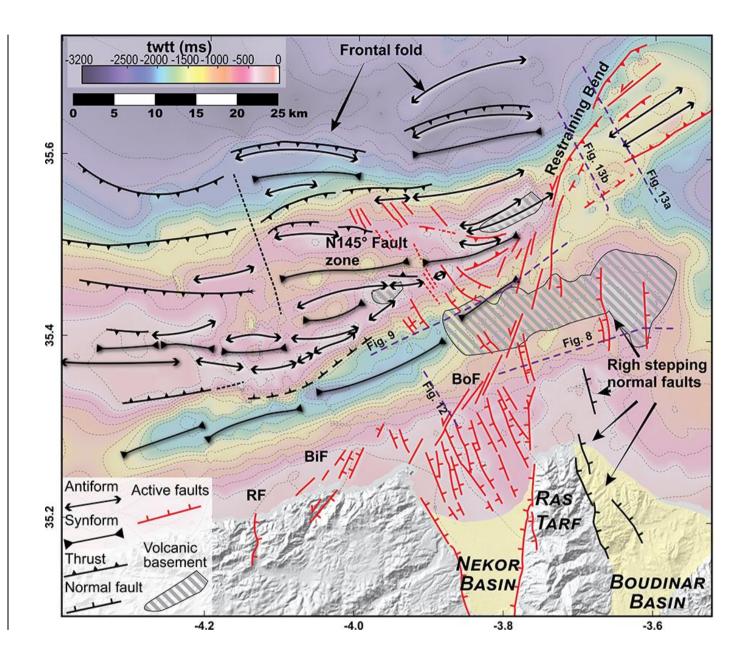


Figure 9. Multichannel seismic profile showing seismic stratigraphy and the main structural elements along a portion of the South Alboran Trough located between N145° striking faults and the AIF. Line track on figure 3. (a) Raw seismic line (b) Interpreted seismic line. Red-crosses in b) figure a seismic body made of poorly continuous high-amplitude reflectors interpreted as volcanoclastic deposits.



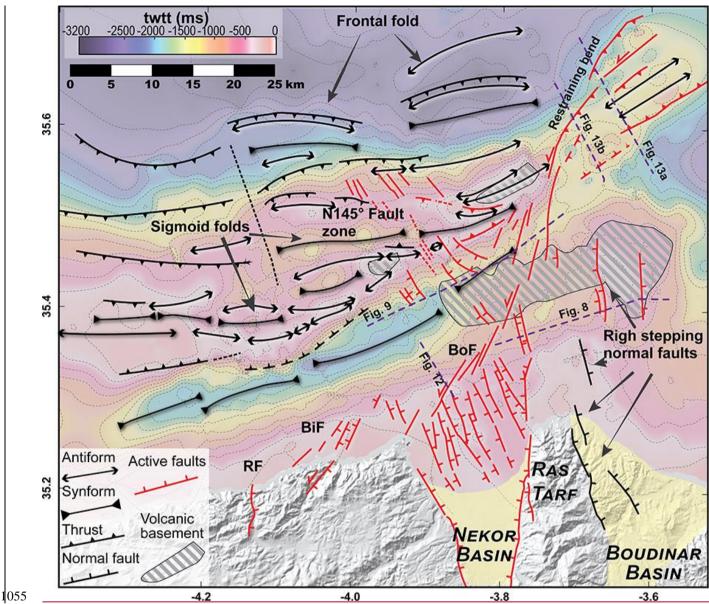
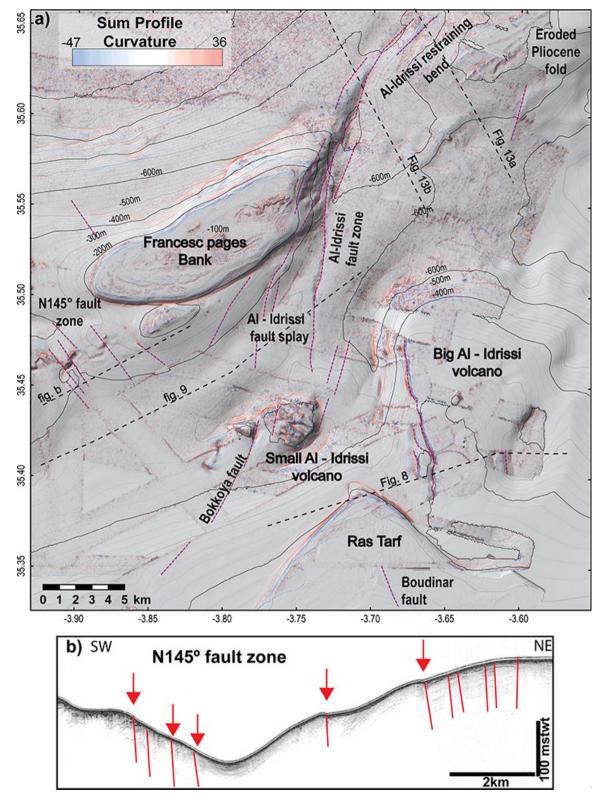
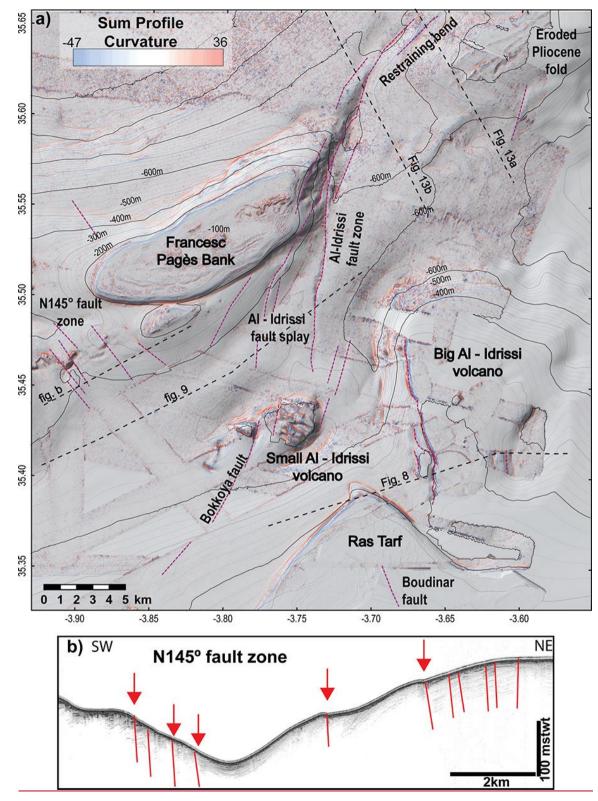


Figure 10: Structural map of Plio-Quaternary faults and folds overlying the map of depths of the Messinian unconformity. Active faults correspond to the faults affecting the seafloor. BF: Boussekkour Fault; Bof, Bokoya Fault; RF, Rouadi Fault.





- 1060 Figure 11: Active structures around the roughly NNE-SSW AIF and adjacent submarine highs. The AIF bends to the North, where it follows the trends of the NAR. High values of curvatures in the Francesc Pagès Bank and the Northeast corner of the map underline the linear features at the seafloor, which corresponds to the truncated Miocene-Pliocene layers. Extreme positive values in red represent concave topography at the seafloor; extreme negative values in blue represent convex topography. a) Profile curvature map textured above the shaded bathymetry; dashed purple lines, fault tracks at the seafloor; dashed black lines, positions of the
- 1065 seismic line in (b) and in figures 8, 9, and 13. b) TOPAS profile showing active N145° normal faults. Red lines, active faults; red arrows, positions of the fault traces in (a).

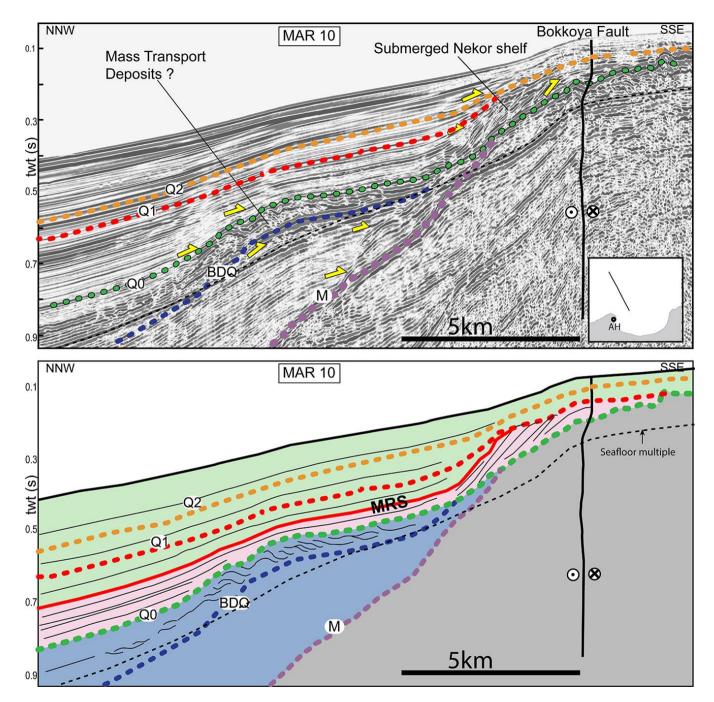
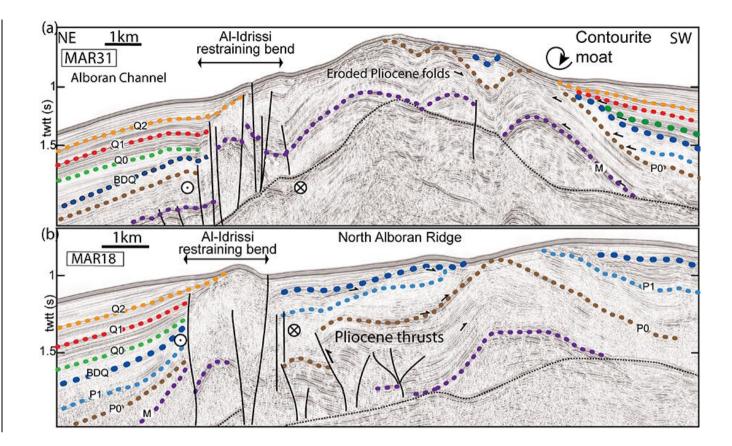


Figure 12: SPARKER seismic line showing the transgression of marine sediment (in green) over the prograding shelf of the Nekor Basin (in pink). Oldest depositional units (Pliocene) are colored in blue and the acoustic basement in grey. The Maximum Regressive Surface (MRS) is in red.



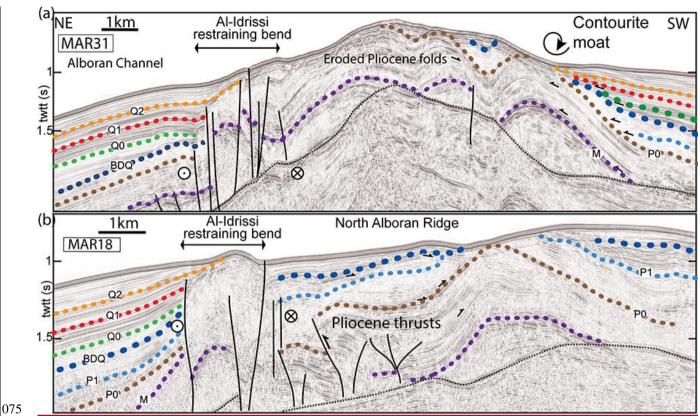


Figure 13: Multichannel seismic lines across the <u>left-lateral</u> restraining bend of the Al-Idrissi fault zone showing lateral evolution of the tectonic structures in North Alboran Ridge and in the <u>left-lateral</u> restraining bend. a) The Al-Idrissi fault zone is a positive flower structure following the front of the Alboran Ridge. b) The Al-Idrissi fault zone is a positive flower structure distinct from the Pliocene thrusts and folds.

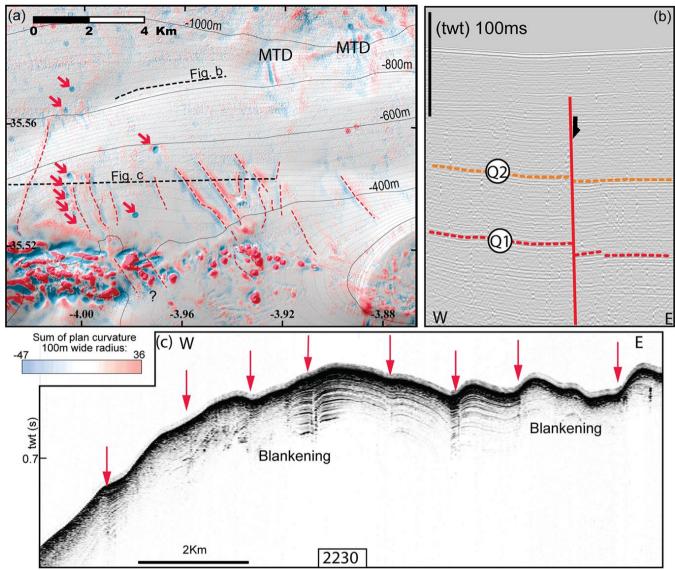
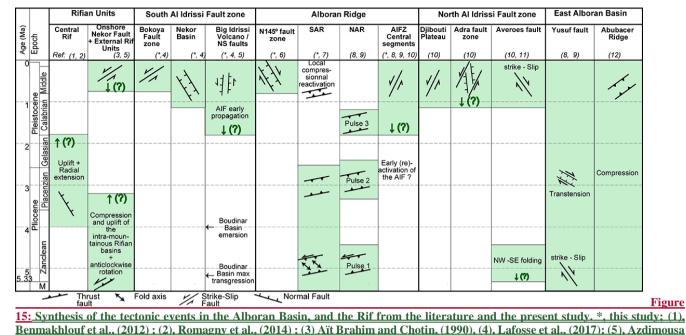


Figure 14: Active structures affecting the northern flank of Francesc Pagès and Ramon Margalef highs. a) plan curvature map overlying the shaded bathymetry; red arrows pockmarks on the seafloor; dashed black lines, seismic lines in the figures (b) and (c); dashed red lines, positions of the fault tracks. b) SPARKER seismic reflection line showing the northward continuity of N145° fault (red line). c) TOPAS seismic line showing the subsurface of the seafloor. Red arrows, positions of the faults drawn in a).



<u>Benmäkniout et al., (2012) ; (2), Komagny et al., (2014) ; (3) Alt Branin and Choun, (1990), (4), Latosse et al., (2017); (5), Azdimousa et al., (2006); (6), Galindo-Zaldivar et al., (2018); (7) Juan et al., (2016); (8) Martínez-García et al., (2013) ; (9), Martínez-García et</u> al., (2017); (10), Gràcia et al., (2019); (11), Perea et al., (2018); (12) Giaconia et al., (2015). The main tectonic events are in green.

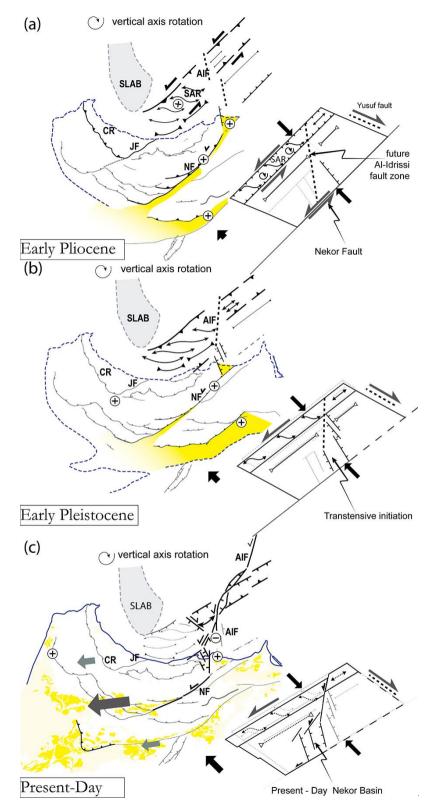
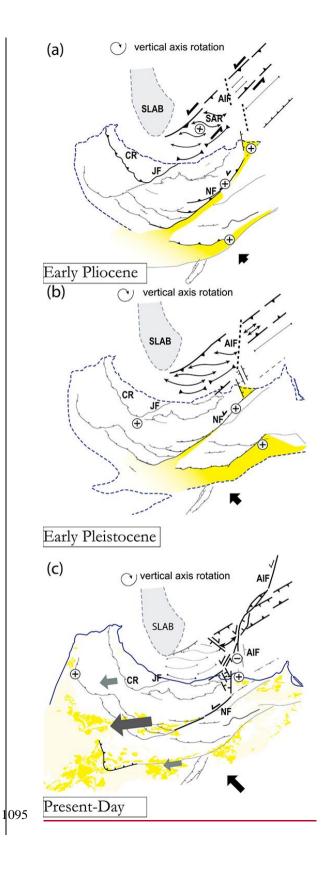


Figure 15Green arrows and question marks indicate the age uncertainties of the main tectonic events.



**Figure 16**: Palinspastic maps of the SAR and the Rif from 5 Ma to the present-day are using 14 ° clockwise rotation of the Alboran tectonic domain from a) to c). Dashed blue line, approximate coastline; continuous blue line, present-day coastline; Dark yellow, Miocene-Pliocene onshore basins; light yellow, Pliocene and Quaternary onshore basins; grey patch, position of the slab remaining approximatively constant below the Alboran Basin during the Plio-Quaternary; left bottom corner of the maps, simplified drawing figure the area between the SAR, the Nekor fault and the Yusuf fault. Thick grey arrows in (c) indicate the direction and relative amount of extrusion in the central Rif considering a fixed Eurasia. The shortening is accommodated through compressive structures in (a). The initiation of subsidence along the Big Al-Idrissi Volcano and the Moroccan shelf corresponds to (b), and the present–day partitioning of the deformation corresponds to (c). CR, central Rif, JF, Jebha Fault; NF, Nekor Fault; AIF, Al-Idrissi Fault zone.